Biol. Cybern. 50, 15–33 (1984)

Biological Cybernetics

Cable Theory in Neurons with Active, Linearized Membranes

Christof Koch

Department of Psychology and Artificial Intelligence Laboratory, Massachusetts Institute of Technology, 545 Technology Square, Cambridge, MA 02139, USA

Abstract. This investigation aims at exploring some of the functional consequences of single neurons containing active, voltage dependent channels for information processing. Assuming that the voltage change in the dendritic tree of these neurons does not exceed a few millivolts, it is possible to linearize the non-linear channel conductance. The membrane can then be described in terms of resistances, capacitances and inductances, as for instance in the small-signal analysis of the squid giant axon. Depending on the channel kinetics and the associated ionic battery the linearization yields two basic types of membrane: a membrane modeled by a collection of resistances and capacitances and membranes containing in addition to these components inductances. Under certain specified conditions the latter type of membrane gives rise to a membrane impedance that displays a prominent maximum at some nonzero resonant frequency f_{max}. We call this type of membrane *quasi-active*, setting it apart from the usual passive membrane. We study the linearized behaviour of active channels giving rise to quasi-active membranes in extended neuronal structures and consider several instances where such membranes may subserve neuronal function: 1. The resonant frequency of a quasi-active membrane increases with increasing density of active channels. This might be one of the biophysical mechanisms generating the large range over which hair cells in the vertebrate cochlea display frequency tuning. 2. The voltage recorded from a cable with a quasi-active membrane can be proportional to the temporal derivative of the injected current. 3. We modeled a highly branched dendritic tree (δ-ganglion cell of the cat retina) using a quasi-active membrane. The voltage attenuation from a given synaptic site to the soma decreases with increasing frequency up to the resonant frequency, in sharp contrast to the behaviour of passive membranes. This might be the underlying biophysical mechanism of receptive fields whose dimensions are large for rapid signals but contract to a smaller area for slow signals as suggested by Detwiler et al. (1978).

1 Introduction

When studying the electrical function of the dendritic tree of nerve cells, it is usually assumed that the membrane impedance can be modeled by a passive membrane, i.e. a resistance in parallel with a capacity. Using such a membrane one can derive, via classical one-dimensional cable theory, the potential within the dendritic tree for various synaptic inputs (for instance Rall, 1977). However, several lines of evidence throw doubt on the generality of the underlying assumption. Recent advances in in-vitro culture techniques and the application of voltage clamp have made it possible to identify a wide variety of voltage-dependent currents distributed throughout the nerve cell. Llinas and Sugimori (1980) found in mammalian Purkinje cells high-threshold Ca^{2+} spikes, believed to originate in the dendritic tree, with different kinetics than the sodium carried somatic spikes. In inferior olivary neurons Llinas and Yarom (1981) likewise recorded high-threshold spikes, mediated by a non-inactivating calcium current distributed in the dendrites (see also Connors et al., 1982; Schwartzkroin and Slawsky, 1977). Wong et al. (1979) observed fast, low-threshold Na^+ and slow, high-threshold Ca^{2+} dendritic spikes in hippocampal neurons. Apart from these all-or-none events several smaller currents in the subthreshold range have been discovered, for instance the rapidly inactivating, K^+ based I_A-current in hippocampal neurons (Gustafsson et al., 1982) and the I_M-current in various vertebrate neurons (Brown and Adams, 1980; Halliwell and Adams, 1982). The I_M-current, a persistent potassium conductance possibly distributed throughout the dendritic tree (Halliwell and Adams,

1982), has been shown to depend not only on voltage, but also on a muscarinic agonist. Thus, the channel responsible for this current depends not only on potential but also on a neurotransmitter (for an excellent review of this new development see Crill and Schwindt, 1983). A large class of potassium channels is activated by an increased level of intracellular Ca^{2+}, thereby possibly linking the cell's metabolism with its membrane conductance (see for instance Adams et al., 1982 in bullfrog sympathetic neurons; Lewis and Hudspeth, 1983 in bullfrog hair cells). In some instances non-spiking neurones, thought unable to generate impulses under normal, physiological conditions, have been shown to possess regenerative properties (see Hengstenberg, 1977 in interneurones of the visual system of the fly; Mirolli, 1981 in motor interneurones of the crab; Johnston and Lam, 1981 in horizontal cells of the teleost retina).

Even if neurons behave linearly within a given voltage range, they need not necessarily be passive. It is known that the membrane of some specialised neurons, like hair cells in the vertebrate cochlea (Crawford and Fettiplace, 1980, 1981), fish electroreceptors (Hopkins, 1976; Meyer and Zakon, 1982) or the rod network in the retina of lower vertebrates (Detwiler et al., 1978, 1980; Torre and Owen, 1983) can best be described by a membrane containing an inductance, in addition to the usual resistance and capacity. Due to this inductance the neuron behaves like a bandpass filter, i.e. its membrane impedance increases with increasing temporal frequency, thereby subserving specific neuronal functions: hair cells show their maximal sensitivity at some frequency value different from zero (Crawford and Fettiplace, 1981; Lewis and Hudspeth, 1983) and rod photoreceptors have a receptive field which increases in size for increased temporal frequency of the stimulus (Detwiler et al., 1978). Even cells which are not nerve cells, like Purkinje fibers of the heart muscle (DeHaan and DeFelice, 1978; Clapham and DeFelice, 1982) or single skeletal muscle fibers (Moore and Tsai, 1983), behave electrically as if their membrane contained inductances. These observations invalidate the concept of a passive dendritic tree whose only function is to integrate the synaptic input and propagate the resulting potential towards the spike-initiation zone near the soma and warrant a new look at the behavioural and functional consequences of active membranes.

In this study, we explore the properties of active, but linearized membranes. Assuming that the voltage change in the dendritic tree does not exceed a few millivolts in magnitude, the non-linear channel conductance can be linearized and described by an electric circuit consisting of several resistances, inductances and capacitances. The full, analytic solution for the spread of excitation in extended neuronal structures with such membranes is only known in two cases: for the infinite squid axon (Sabah and Leibovic, 1969; Mauro et al., 1970; Sirovich and Knight, 1977) and for a one- or two-dimensional network of discrete rodes, each one modeled by a RLC circuit (Torre and Owen, 1983; Torre et al., 1983). Using a recently developed algorithm (Koch and Poggio, 1983b) we study properties of cables and branched trees endowed with a linearized membrane, placing special emphasis on their role in information processing.

2 The General Solution of the Cable Equation

The main topic of the present analysis is the electric behaviour of membranes containing active, voltage- and time-dependent channels for voltage values not too far away from the resting potential of the cell. Within this voltage range, which depends strongly on the density of the channels, the conductance of the channel can be linearized to yield phenomenological inductances, capacitances and resistances. To be able to study the propagation of voltage in extended neuronal structures with an arbitrary linear membrane we have proposed a representation of such structures in frequency space together with a simple algorithm to generate the solution of the corresponding cable equation (Koch and Poggio, 1983b).

2.1 Linear Cable Theory

Denoting the linearized, frequency-dependent membrane impedance by $z_m(\omega)$ and the serial impedance by $z_a(\omega)$ we represent a linear, one-dimensional cable as an infinite ladder network illustrated in Fig. 1[1]. Since we can safely model the serial impedance as a purely ohmic resistance r_a (for a discussion of this, see Scott, 1972), we will henceforth always assume that $z_a(\omega)=r_a$. For a passive membrane $z_m(\omega)$ is given by

$$z_m(\omega)=\frac{r}{1+i\omega\tau}, \tag{1}$$

where τ is the membrane time-constant $\tau=rc$, and c the membrane capacity. Under the basic assumptions of one-dimensional cable theory (for a review see Rall, 1977) we write the cable equation directly in the Fourier domain as

$$\frac{\partial^2\tilde{V}(x,\omega)}{\partial x^2}=\gamma(\omega)^2\tilde{V}(x,\omega), \tag{2}$$

where $\tilde{V}(x,\omega)$ is the Fourier transform (with respect to time) of the membrane potential $V(x,t)$ at x and $\gamma(\omega)$ is

1 ω is related to the frequency f by $\omega=2\pi f$

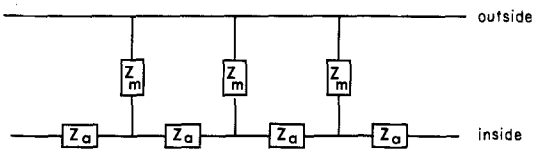

Fig. 1. The general representation of a one-dimensional cable with an arbitrary frequency-dependent membrane impedance $z_m = z_m(\omega)$ and serial impedance $z_a = z_a(\omega)$

the propagation constant defined by

$$\gamma(\omega)^2 = \frac{z_a(\omega)}{z_m(\omega)} \tag{3}$$

(for a derivation see Koch and Poggio, 1983b). Equation (3) shows the advantage of using the Fourier transform $\tilde{V}(x, \omega)$ instead of the original function $V(x, t)$. For the latter case, finding the voltage in a cable with a membrane containing a capacity, a resistance and an inductance in parallel entails solving a partial differential equation of order two in space and three in time, while the corresponding Eq. (2) is a simple second order differential equation. The nature of the neuronal membrane is fully contained in $\gamma(\omega)$ and does not affect the form of Eq. (2). Solving Eq. (2) for an infinite cable if a δ-current impulse is injected at the origin and the voltage is recorded at a distance x farther away[2], subject to the boundary condition that $\tilde{V}(x, \omega)$ tends to zero as x tends to infinity, leads to the solution

$$\tilde{V}(x, \omega) = \frac{0.5 r_a}{\gamma(\omega)} e^{-x\gamma(\omega)} \tag{4}$$

(see Koch, 1982). Because a cable with a linear membrane is a linear system (if currents are used as inputs), we introduce the Green function $K(x, t)$, i.e. the response of the system to a δ-input impulse. Considering the Fourier transform of the Green function, that is the transfer function $\tilde{K}(x, \omega)$, we identify the transfer function (or transfer impedance) with the voltage from (4):

$$\tilde{K}(x, \omega) = \frac{0.5 r_a}{\gamma(\omega)} e^{-x\gamma(\omega)}. \tag{5}$$

If the voltage is recorded at the site where the current is injected, we obtain the familiar input impedance

$$\tilde{K}(0, \omega) = 0.5 r_a \gamma(\omega)^{-1}. \tag{6}$$

The voltage response at x for arbitrary current inputs $\tilde{I}(\omega)$ can now be determined via the convolution theorem:

$$\tilde{V}(x, \omega) = \tilde{K}(x, \omega) \cdot \tilde{I}(\omega). \tag{7}$$

In a few cases it is possible to derive directly the time course of the impulse response [i.e. $K(x, t)$]. The temporal behaviour of the light response in the discrete two-dimensional network of rod photoreceptors can for instance be obtained explicitely if the poles and zeros of $z_m(\omega)$ are known (Torre and Owen, 1983; Torre et al., 1983).

2.2 The Frequency-Dependent Space Constant

Another variable of interest is the generalized, frequency-dependent space or length constant $\lambda(\omega)$, defined as the distance over which a sinusoidal voltage of frequency ω decays to $1/e$ of its original value (Eisenberg and Johnson, 1970).

$$\frac{1}{\lambda(\omega)} = \mathrm{Re}\{\gamma(\omega)\}, \tag{8}$$

where $\mathrm{Re}\{z\}$ indicates the real part of the complex number z. In a cable with a passive membrane $\lambda(\omega)$ is, just as $\tilde{K}(x, \omega)$, a monotonic decreasing function of frequency, since at higher frequencies more and more charge leaks through the membrane capacity. Under certain conditions, however, $\lambda(\omega)$ shows a pronounced maximum at some non-zero frequency value, leading to an increased spread of voltage at this frequency in comparison with lower or higher frequency components (see also Clapham and DeFelice, 1982; Torre and Owen, 1983).

Since we are only concerned with the modulus (or amplitude) and not the phase of the transfer function, we combine Eqs. (5), (6), and (8) into

$$|\tilde{K}(x, \omega)| = |\tilde{K}(0, \omega)| e^{-x/\lambda(\omega)}. \tag{9}$$

2.3 Classification of Membranes Types

To analyse the different electrical properties of linear membranes we find it helpful to distinguish between different types of membranes. A *purely passive* membrane can be modeled by a leakage resistance in parallel with a membrane capacity, the usual assumed RC configuration. *A generalized passive* membrane consists of a RC circuit in addition to other electrical elements like resistances, capacitances and even inductances as long as the associated membrane impedance $z_m(\omega)$ decreases with increasing frequency. Therefore, the generalized passive membrane will always behave as a lowpass filter. In a specific instance it might be very difficult to distinguish experimentally between a purely passive RC circuit and a generalized lowpass membrane. The *quasi-active* membrane shows bandpass-like behaviour with a prominent maximum in its membrane impedance. Such a membrane must contain a large phenomenological inductance. By exclusion we define as *active* membranes all membranes which behave non-linearly with respect to membrane voltage, whether spiking or non-spiking.

2 Note that x, defined as a distance, is always positive

3 The Existence and Properties of Phenomenological Inductances

3.1 When Does an Inductance-like Element Arise?

To study the behaviour of the transfer function $\tilde{K}(x, \omega)$, relating it to the underlying membrane impedance $z_m(\omega)$, we consider first under what conditions a phenomenological inductance arises. As Detwiler et al. (1980) have pointed out, an inductance can be realized by a time- and voltage-dependent K^+ conductance activated by depolarization and inactivated by hyperpolarization. Examples are the currents mediated by potassium channels in the squid giant axon (Hodgkin and Huxley, 1952) or in the cat motoneuron (Barrett et al., 1980) or by the Ca^{2+} triggered K^+ current in sympathetic neurons and hair cells of the bullfrog (Adams et al., 1982; Lewis and Hudspeth, 1983). Alternatively, an inductance can mimic the small-signal behaviour of the time- and voltage-dependent Na^+ (or Ca^{2+}) conductance activated by hyperpolarization and deactivated by depolarization as for instance the low-threshold calcium mediated ionic current in mammalian CNS neurons (Llinas and Yarom, 1981; Llinas and Jahnsen, 1982). Note that the threshold at which a given current generates spike-like components is proportional to the range of validity of the linear description.

3.2 Bandpass Behaviour of Quasi-active Membranes

It is well known from electric circuit theory that the presence of an inductance can lead to resonant behaviour, i.e. the voltage leads the current (positive phase) for a certain range of frequency values while the impedance shows a maximum. In trying to answer the question when resonant behaviour in linearized membranes occurs, we introduce the two following definitions: The complex function $\tilde{K}(\omega)$ is said to be a bandpass if the amplitude of $\tilde{K}(\omega)$ increases continuously from its minimum at $\omega=0$ until it peaks at some positive frequency. The value of ω at which this maximum is attained is known as the resonant frequency $\omega_{max}=2\pi f_{max}$. Because we always assume the presence of the membrane capacity c, which acts as a shunt at high frequencies, $\tilde{K}(\omega)$ tends to zero as $\omega \to \infty$ [3]. To characterize the quality of a bandpass, we define q as the ratio of the amplitude of $\tilde{K}(\omega)$ at its resonant frequency to the steady-state value (which is always real)

$$q=\frac{|\tilde{K}(\omega_{max})|}{\tilde{K}(0)}. \tag{10}$$

3 During all our simulations we have never seen a function with more than one extremum

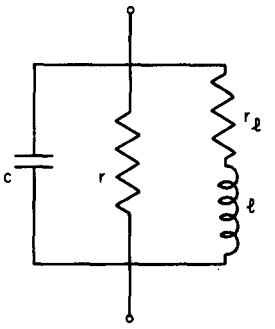

Fig. 2. The electrical representation of a quasi-active membrane modeled by a passive component (leakage resistance r in parallel with a capacity c) in addition to an inductive branch. This branch, made up by an inductance l in series with a resistance r_l, describes on a phenomenological level the electrical behaviour of a specific type of active channel for small variations of voltage around a fixed potential $\bar{V}$

One requirement for a true bandpass-filter is $q>1$, i.e. the impedance at the resonant frequency should be larger than the steady-state impedance. Using these definitions we can tackle the problem under what conditions the membrane impedance shows a resonant maximum. Consider the simplified membrane shown in Fig. 2, consisting of an RC-element in parallel with an inductive branch, arising from a small-signal analysis of some active channel. For this system it can be proved rigorously (see Appendix I) that within a range of values for the inductive resistance r_l – extending from 0 to some finite positive value of r_l – the membrane impedance $z_m(\omega)$ increases monotonically from $\omega=0$ up to its resonant frequency. Subsequently the impedance drops to zero. Therefore, within this range of r_l, $q>1$. For the ideal resonant circuit, i.e. $r_l=0$, the system resonates at the characteristic frequency $f_{max}=(lc)^{-1/2}$. Increasing r_l leads first to an increase in ω_{max} and then to a slow decrease until ω_{max} merges with the extremum at $\omega=0$, changing $z_m(\omega)$ from a bandpass into a lowpass. ω_{max} can be shifted towards greater frequency values by decreasing the leakage resistance r. Beyond the before mentioned range of r_l-values, the resistance is too large to allow the circuit to resonate and $z_m(\omega)$ is always a lowpass. The same also applies to the leakage resistance r: if it is small enough $z_m(\omega)$ will always be a bandpass. In the general situation of an arbitrary impedance $z_m(\omega)$ in parallel with an inductive branch, the combined impedance always exhibits a maximum for small enough values of the inductive resistance r_l (Appendix I).

Given that $z_m(\omega)$ does indeed show bandpass-behaviour, we prove the following proposition (for a detailed proof see Appendix II):

Theorem. *Bandpass behaviour of a linear, infinite cable. If the membrane impedance $z_m(\omega)$ is a bandpass in the*

above sense, it follows that in an infinite cable of constant diameter

the input impedance $\tilde{K}(0,\omega)$ is a bandpass with the same resonant frequency as the membrane impedance and vice versa,

the transfer impedance $\tilde{K}(x,\omega)$ for any x is a bandpass,

the generalized length constant $\lambda(\omega)$ is a bandpass

(for the last two points the converse, unfortunately, does not hold).

In other words, if a small patch of membrane behaves as a bandpass, so does the transfer function of the whole cable and the space constant. Accordingly, a sinusoidal voltage in such a cable will tend to propagate farthest if its frequency is in a neighbourhood of ω_{max}.

4 The Existence and Properties of Phenomenological Capacitances

4.1 When Does a Capacity-like Element Arise?

Up to now we have only been concerned with the existence and the consequences of an inductive branch arising out of the linearization of an active, voltage-dependent channel. But under what conditions does a capacitive branch (in addition to the passive RC-element) arise and what are its functional consequences? Basically, a voltage-dependent conductance mimics a capacitive branch (consisting of a capacity c_c in series with a resistance r_c) if the current behaves like $I = c_c \frac{\partial V}{\partial t} + \frac{V}{r_c}$. This is the case when the Na^+ (or Ca^{2+}) conductance is activated by depolarization as during the rising phase of the fast, Na^+ spike or for the high-threshold, non-inactivating Ca^{2+} conductance (Llinas and Sugimori, 1980; Llinas and Yarom, 1981; Schwartzkroin and Slawsky, 1977; Lewis and Hudspeth, 1983) or when a voltage-dependent K^+ conductance decreases for depolarization and increases with hyperpolarization.

4.2 Temporal Delays in a Lowpass Membrane

In what way does the existence of such an extra capacitance influence the behavior of the membrane? Adding to a lowpass membrane an additional capacitive branch does not change the fundamental nature of the membrane, i.e. its decreasing impedance for increasing frequency, even if such a circuit cannot be reduced to the usual RC configuration. What changes is the time-constant of the system, which increases by adding a capacitive branch. Such an increased response time might be useful for various types of neuronal signaling (for instance for movement detection; Reichardt, 1961; Torre and Poggio, 1978). The notion of a delay incurred by a signal passing through a cable can be made more precise by introducing the phase-time-lag $t_\phi(\omega)$ defined as the time it takes a sinusoidal input signal of frequency ω to pass through the system. It can be shown that the phase-time-lag in an infinite cable with propagation constant $\gamma(\omega)$ [Eq. (3)] is given by

$$t_\phi(\omega) = \frac{1}{\omega} \operatorname{arctg} \frac{\operatorname{Im}\{\gamma(\omega)\}}{\operatorname{Re}\{\gamma(\omega)\}} + \operatorname{Im}\{\gamma(\omega)\} \frac{x}{\omega} \qquad (11)$$

(see Koch, 1982; Brühl et al., 1979)[4]. Introducing a capacitive branch does indeed increase $t_\phi(\omega)$ but with the undesirable side effect of decreasing the space constant $\lambda(\omega)$, since more charge leaks through the membrane than before. Another way to enhance delays is by increasing the leakage resistance r which concomitantly raises $\lambda(\omega)$.

To illustrate this we model a membrane consisting of a RC-element in parallel with a capacitive branch using the following parameters: $r = 3333\,\Omega\,cm^2$; $c = 1\,\mu F\,cm^{-2}$; $r_c = 2300\,\Omega\,cm^2$; $c_c = 1\,\mu F\,cm^{-2}$. The phase-delay in an infinite cable (of 1 µm diameter) when recording the voltage at the site of current injection decreases from its peak value $t_\phi = 3.3$ ms for stationary inputs to 0.2 ms at 500 Hz. If the voltage is recorded one steady state space constant (345 µm) farther away, t_ϕ decreases from 6.6 ms to 0.7 ms. Over the same temporal frequency range the space constant drops from its maximum $\lambda_0 = 345\,\mu m$ to 140 µm. We compared these numbers with the phase-time in an infinite cable with a purely passive membrane with a three-fold increased leakage resistance; i.e. $r = 10{,}000\,\Omega\,cm^2$; $c = 1\,\mu F\,cm^{-2}$ and no additional capacitive branch. Now the phase-time associated with the input impedance measurement drops from 5.0 ms to 0.25 ms while the corresponding values for the transfer function are 7.9 and 0.7 ms. Simultaneously, the space constant is reduced from its maximal steady-state value $\lambda_0 = 598\,\mu m$ to 150 µm at 500 Hz.

After considering the specific properties of the basic types of linear membranes, we will now focus on one particular instance of such a membrane: the membrane derived by linearizing the Hodgkin-Huxley equations for the unmyelinated squid axon.

5 The Linearized Hodgkin-Huxley Equations

5.1 General Properties of the Linearized, Hodgkin-Huxley Membrane

The distribution of the membrane voltage in an axon (or dendrite) is described by the partial differential

4 For more details on the time-lag and on a precise method of assessing the velocity of PSP's in cables with an arbitrary linear membrane see Koch and Poggio (1984)

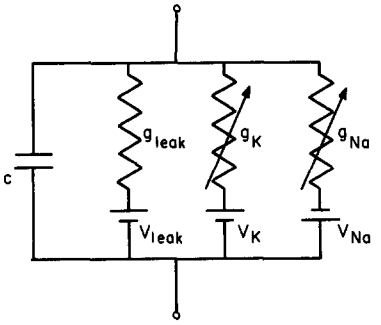

Fig. 3. The electrical circuit representing a small patch of membrane in the unmyelinated squid axon (Hodgkin and Huxley, 1952). Note that the usual passive membrane component (i.e. c and $g_{leak}=1/r_{leak}$) are time- and voltage-invariant

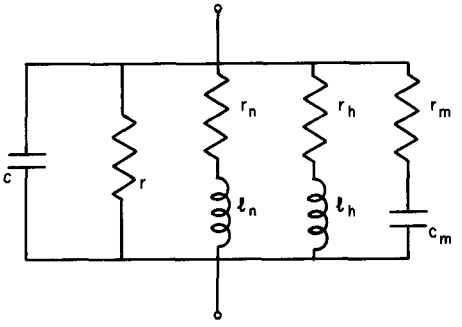

Fig. 4. The equivalent RLC circuit of a small patch of membrane of the type shown in Fig. 3 for small variations of voltage. Linearizing the Hodgkin-Huxley equations around any value of the membrane potential $\bar{V}$ between V_K and V_{Na} gives always a qualitative similar type of circuit. For the values of the electrical elements see Appendix III

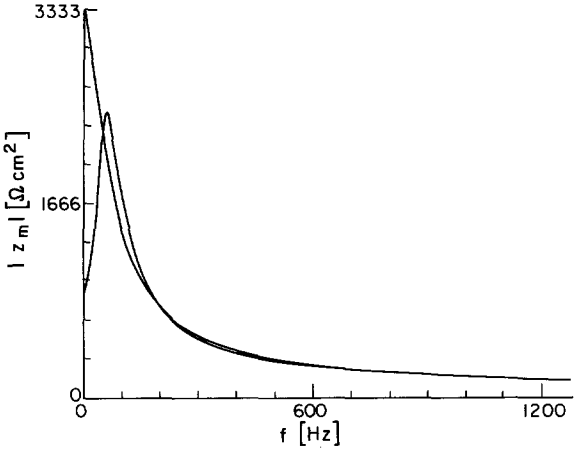

Fig. 5. The membrane impedance z_m for two types of membranes as a function of frequency. Calculating the amplitude of the impedance of the quasi-active membrane shown in Fig. 4 gives rise to the bandpass-like function which increases from its steady-state value 857 Ω cm² to its peak 2422 Ω cm² at 67 Hz. This corresponds to a q of 2.83. Reducing the density of active, voltage-dependent channels to zero leads to a purely passive membrane with a monotonically decreasing impedance $z_m(\omega)$. In both cases is $r_{leak}=3333\,\Omega\,\mathrm{cm}^2$ and $c=1\,\mu\mathrm{F\,cm}^{-2}$. Note that beyond 200 Hz both curves coincide

equation

$$\frac{1}{r_a}\frac{\partial^2 V(x,t)}{\partial x^2}=c\frac{\partial V(x,t)}{\partial t}+I_i(t). \tag{12}$$

The current $I_i(t)$ carried by the movements of ions through the membrane is the sum of the currents due to different ion-specific channels. Hodgkin and Huxley formulated (1952) a mathematical model of the squid axon using four independent variables V, m, n, and h:

$$I_i(t)=\bar{g}_{Na}m^3h(V(t)-V_{Na}) + \bar{g}_K n^4(V(t)-V_K)+g_{leak}(V(t)-V_{leak}), \tag{13}$$

where m, h, and n describe the sodium activation, the sodium inactivation and the potassium activation as a function of time and voltage (Fig. 3). The behaviour of these variables is regulated by three first-order differential equations [Eq. (AIII.2)]. Linearizing these equations for small variations of voltage δV around the membrane potential $\bar{V}$ yields a total, phenomenological membrane impedance for subthreshold responses equivalent to three RL branches in parallel: two with positive and one with a negative resistance (for an exact description of the resulting membrane see Appendix III). The branch with the negative resistance mimics the m process of the sodium activation while the other two branches are equivalent to the inactivation process of the Na^+ current and to the activation of the K^+ current. However, the negative RL branch can be converted into a RC branch with a positive value of the resistance [Eq. (AIII.4)]. The true membrane capacity and leakage resistance act in parallel with these phenomenological elements to give a total impedance $z_m(\omega)$ which is, in effect, a parallel RLC configuration (Fig. 4):

$$z_m(\omega)=\frac{\beta_3(i\omega)^3+\beta_2(i\omega)^2+\beta_1(i\omega)+\beta_0}{\alpha_4(i\omega)^4+\alpha_3(i\omega)^3+\alpha_2(i\omega)^2+\alpha_1(i\omega)+\alpha_0} \tag{14}$$

with the constants α_i and β_i depending on the value of the electrical elements [see Mauro et al. (1970) or Sabah and Leibovic (1969) for an assessement of the quality of the linear approximation]. The existence of these inductances in the membrane of the squid axon were first reported by Cole and Baker (1941; see also Cole, 1941). The membrane impedance, plotted in Fig. 5, increases from the steady state value up to the resonant frequency at 67 Hz, tending subsequently to zero as the frequency increases. Also shown is $z_m(\omega)$ for a passive membrane with the same leakage resistance as in the quasi-active case but in the absence of any active channels [i.e. $\eta\to 0$; Eq. (15)]. Beyond 200 Hz the two curves overlap substantially. Thus both types of membranes show similar electrical behavior if events changing on the time scale of one or 2 ms or faster are

considered. The distinct electrical properties of these linearized membranes are therefore due to the fact that $z_m(\omega)$ increases from 0 to f_{max} for the quasi-active membrane but decreases in the passive case.

But when is linearization permittable and when does it lead to instabilities, i.e. a finite input resulting in a diverging output? The denominator of $z_m(\omega)$ [Eq. (14)], a fourth degree polynomial in ω, is in fact the characteristic equation for the linearized system. The response of the linear system will always be of the form

$$V(t) = \sum_{i=1}^{4} C_i e^{\lambda_i t},$$

where the C_i are constant and the λ_i the roots of the characteristic equation. If the real part of each root λ_i is less or equal to zero, all perturbations δV from the potential $\bar{V}$ tend to decrease with time and the point $\bar{V}$ is stable (Chandler et al., 1962). If at least one root has a positive real part, the system has run-away solutions and is therefore unstable. To investigate the stability of the system without solving explicitly for the roots we used the algebraic Routh-Hurwitz criterion (Korn and Korn, 1961), consisting of 6 inequalities in the α_i's. One of these requirements is that the total steady-state resistance (i.e. $1/r + 1/r_n + 1/r_h$) be positive. Varying $\bar{V}$ between V_K and V_{Na} and assuming standard Hodgkin-Huxley parameters (see Appendix III) we find, in excellent agreement with values reported in the literature (Sabah and Spangler, 1970) that the Routh-Hurwitz criterion fails to be satisfied at $\bar{V}_{crit} = 5.35$ mV. Around $\bar{V} = 3.18$ mV the shunting resistance r diverges to $+\infty$, subsequently changing sign and decreasing in amplitude, i.e. from $-\infty$ to finite, negative values. If a current that increases sufficiently slowly is applied to the nonlinear membrane, the system displays subthreshold oscillations at $V = \bar{V}_{crit}$ (Cooley and Dodge, 1966; Sabah and Leibovic, 1969; see also Rinzel, 1978). Since the voltage threshold for eliciting a spike in the nonlinear system is above this value, we conclude that the instability of the linear system does not necessarily imply spiking behaviour of the nonlinear system (see also Fig. 10).

5.2 *The Impulse Response in an Infinite Cable*

Figure 6 shows the amplitude of the input impedance $\tilde{K}(0, \omega)$ and transfer impedance $\tilde{K}(x, \omega)$ for $x = 2\lambda_0$, i.e. twice the steady state space constant, in an infinite axon of constant diameter and with the same membrane as in Fig. 4. In Fig. 7 we have plotted the corresponding Green functions $K(0, t)$ and $K(x, t)$ obtained by applying the inverse Fourier transform. Due to the bandpass nature of the membrane, both functions show an oscillatory component in the computed

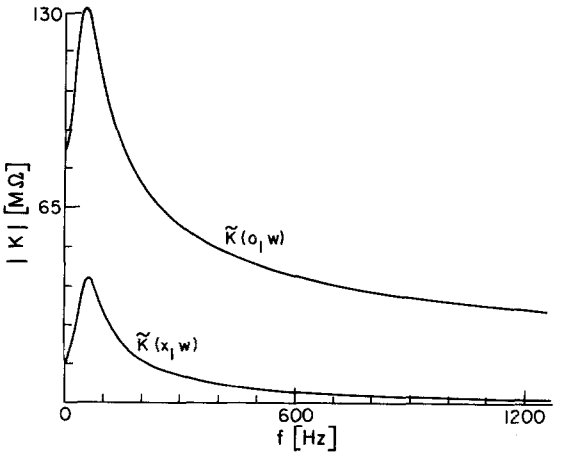

Fig. 6. The amplitude of the input-impedance $\tilde{K}(0, \omega)$ and the transfer impedance $\tilde{K}(x, \omega)$ in an infinite cable of constant diameter ($d = 1\,\mu$m) endowed with the quasi-active membrane shown in Fig. 4. The distance between the site of the current injecting electrode and the voltage recording electrode is two steady state space constants (Fig. 9), i.e. $x = 2\lambda_0 = 350\,\mu$m. The impedance for stationary inputs for $\tilde{K}(0, \omega)$ [respectively $\tilde{K}(x, \omega)$] is 72.98 MΩ (respectively 10.55 MΩ) and increases until 67 Hz (respectively 70 Hz) where it peakes at 131.09 MΩ (respectively 40.67 MΩ). Thus $q = 1.68$ (respectively 3.85). While the shape of $\tilde{K}(0, \omega)$ is independent of the diameter [in fact $\tilde{K}(0, \omega)$ is proportional to $d^{-3/2}$], $\tilde{K}(x, \omega)$ is not. For the same cable with $d = 0.1\,\mu$m or $10\,\mu$m, q is 23.35 or 2.18 while the resonant frequency decreases from 72 to 67 Hz

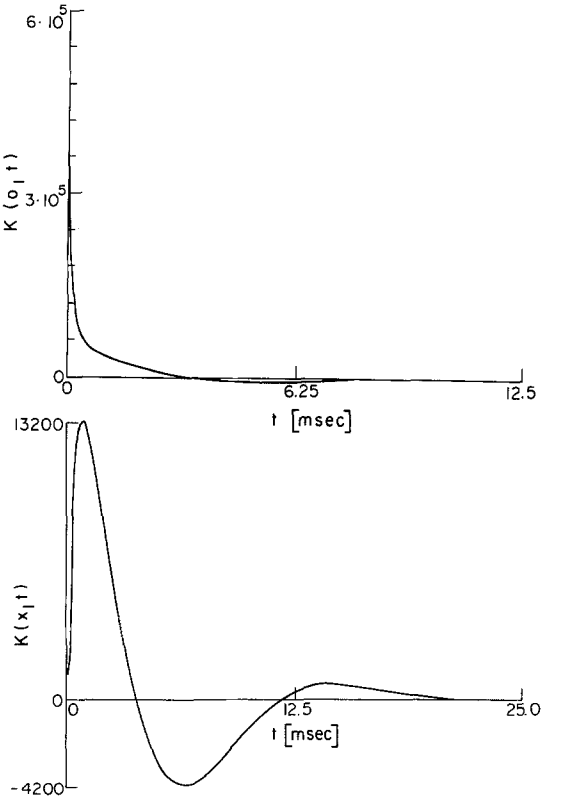

Fig. 7. The Green functions $K(0, t)$ (top) and $K(x, t)$ (bottom) obtained by inverting the corresponding transfer functions of Fig. 6 using the fast Fourier transform. These functions can be thought of as the voltage response of the system to a δ-pulse of current injected at the site of voltage recording or $350\,\mu$m farther away

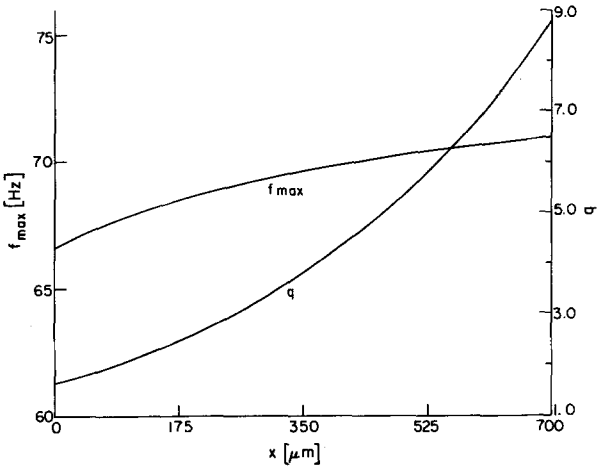

Fig. 8. The resonant frequency f_{max} and q, the ratio of $\tilde{K}(x, f_{max})$ to $\tilde{K}(x,0)$, of the transfer function in an infinite cable (see Fig. 6) as a function of the distance x between the sites of current input and voltage output. f_{max} and q were obtained by numerically evaluating expression (5). q can be approximated very closely by the function $q=1.68e^{0.4156x}$ (coefficient of determination $r^2=0.99998$); $\lambda_0=175\,\mu m$

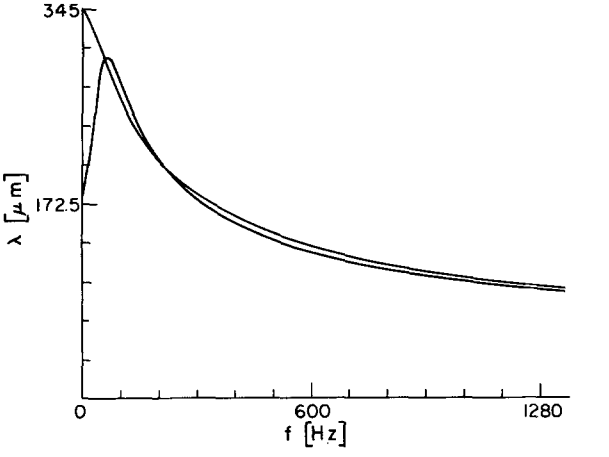

Fig. 9. The frequency dependent space constant $\lambda(\omega)$ in an infinite cable of constant diameter (1 μm) for a passive and a quasi-active membrane (see Fig. 5). $\lambda(\omega)$ increases in the quasi-active case from its steady-state value $\lambda_0=175.0\,\mu m$ to its peak value of 300.4 μm at 74 Hz, while $\lambda(\omega)$ for a passive membrane decreases monotonically from the stationary value $\lambda_0=345.0\,\mu m$. Note that beyond 200 Hz both curves overlap almost completely

response to a impulse current, first de- and then hyperpolarizing. Increasing the distance between the locations of current injection and voltage recording does not have any profound influence on the resonant frequency as demonstrated in Fig. 8. It does, however, lead to an exponential increase in q, the ratio of $\tilde{K}(x, \omega_{max})$ to $\tilde{K}(x,0)$. In fact, this curve can be fitted to a high degree of approximation by a single exponential function: $q=ae^{bx}$. This increase in the "quality" of the bandpass is counterbalanced by the attenuation of the whole transfer function for increasing distances due to charge leaking through the membrane.

Figure 9 shows the frequency dependent space constant $\lambda(\omega)$ for the passive and the quasi-active membrane. Note that $\lambda(\omega)$ scales according to $d^{1/2}$, where d is the diameter of the cable. Due to the presence of channels that decrease the total ohmic membrane resistance, $\lambda(\omega)$ is smaller in the quasi-active case than for the passive membrane and shows a pronounced maximum at 74 Hz.

5.3 Variation of the Shape of the Bandpass with Changing Biophysical Parameters

As we have seen above, the resonant frequency can be shifted (albeit, only slightly) by varying x. A different way to influence ω_{max} is to change directly the electric elements of the circuit making up the membrane. We consider in particular a variable potassium and sodium channel density. Assuming that the conductance of a single channel remains constant and only the density of both Na^+ and K^+ channels change, we replace the expression for the sodium and potassium conductance per unit area $\bar{g}_{Na}$ and $\bar{g}_K$ by

$$g_{Na}=\bar{g}_{Na}\eta, \tag{15a}$$

$$g_K=\bar{g}_K\eta. \tag{15b}$$

Substituting g_{Na} and g_K into the expression for the circuit elements of the linearized membrane, it follows that r_n, r_m, r_h, and c_m are inversely proportional to the channel density η while the specific inductances l_n and l_m are proportional to η [the time constants of the two inductive branches τ_n and τ_h, are therefore insensitive to any changes in η; Eqs. (AIII.3)–(AIII.8)]. By lowering or enhancing η we mimic a decrease or an increase of membrane excitability (see Holden and Yoda, 1981; or Sabah and Leibovic, 1972; who studied the effect of changing η upon the travelling solution of the Hodgkin-Huxley equations in an infinite cable).

Figure 10 shows the numerically determined value of the holding potential $\bar{V}$ at which the linearization procedure leads to an unstable system (V_{crit}) as a function of the channel density for the membrane patch situation. Note that a negative value of $\bar{V}$ always yields a stable system. If η drops below 18.5% of the standard density the linear system is always stable for values of $\bar{V}$ between V_{Na} and V_K. Within the range of η shown in Fig. 10, we could never correlate the first appearance of instability with any obvious or drastic changes in the values of the circuit elements, such as the total steady state impedance of the membrane becoming negative. For all values of η for which the distinction between a decremental response and a

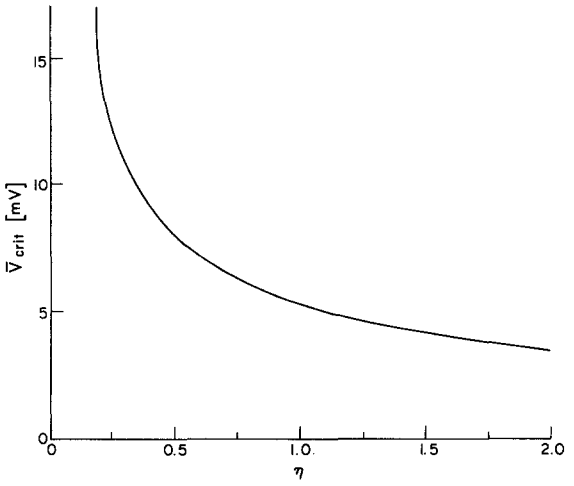

Fig. 10. The numerically determined relationship between $\bar{V}_{crit}$, the holding potential for which the linear system is unstable (relative to the resting potential of the neuron), and the channel density η. Linearization of the channel conductance around $\bar{V}$ is possible if $\bar{V} < \bar{V}_{crit}$. Note that in some cases there exists a second region of stability beyond $\bar{V}_{crit}$. For $\eta = 1$ linearization is possible if $\bar{V} < 5.345$ mV or $\bar{V} > 21.942$ mV (Sabah and Spangler, 1970). Below a channel density of 18.5%, i.e. below a Na^+ channel density of 0.0220 S cm^{-2} and a K^+ channel density of 0.0066 S cm^{-2}, the linear system is stable for values of $\bar{V}$ between V_K and V_{Na}. Generating a spike in the nonlinear Hodgkin-Huxley system with a very short voltage pulse requires a voltage amplitude above $\bar{V}_{crit}$

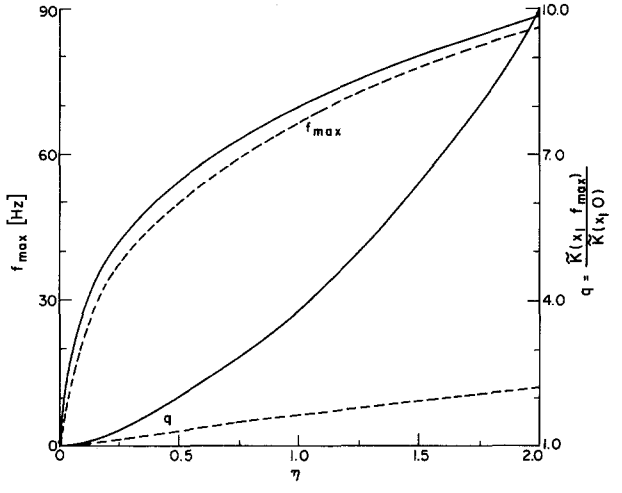

Fig. 11. The resonant frequency f_{max} and q for the input impedance $\tilde{K}(0, \omega)$ (dashed lines) and transfer impedance $\tilde{K}(x, \omega)$ (continuous lines) from Fig. 6 as a function of the channel density. In both cases the best fit to q is an exponential: $q = 1.02e^{0.4347\eta}$ for $\tilde{K}(0, \omega)$ and $q = 1.08e^{1.1811\eta}$ for $\tilde{K}(x, \omega)$

spike was not blurred, the voltage threshold for very fast voltage pulses was always above $\bar{V}_{crit}$.

Figure 11 shows q and f_{max} for $\tilde{K}(0, \omega)$ and $\tilde{K}(x, \omega)$ as a function of the channel density. Notice that as the channel density goes to zero, $\tilde{K}(x, \omega)$ always retains its bandpass properties, i.e. $f_{max} \to 0$ and $q \to 1$. The dependance of q on η can again be fitted accurately by a single exponential function: $q = e^{c\eta}$ with a positive constant c. Combining this approximation with the earlier one yields $q = \text{const} \cdot e^{c\eta + bx}$. Increasing either the distance between input and output or the channel density increases therefore the "quality" of the bandpass.

In summary, the behaviour of these bandpass like filters can be controlled in different ways: by varying the diameter of the cable, the distance between the site of current injection and voltage recording or the density or the type of active channels. While f_{max} is, for a given type of channel, mainly susceptible to changes in channel density, q is an exponential function of both distance and density. Other parameters which we did not consider specifically but which will certainly influence the resonant frequency are the holding potential $\bar{V}$, the temperature and the intra- and extra-cellular concentration of such ions as Ca^{2+} or K^+. In fact, Lewis and Hudspeth (1983) have observed that the frequency of voltage oscillations in isolated bullfrog hair cells, induced by injecting currents, increases with increasing levels of depolarization.

At this point we have to emphasize again that the linearized description of the channel impedance is only valid for a range of voltage values around $\bar{V}$ anywhere between 1 and 10 or 15 mV. Decreasing the channel density η or modeling a channel with a high threshold such as the non-inactivating calcium current (Llinas and Sugimori, 1980; Llinas and Yarom, 1981) leads to an increased range of validity for the linear model.

We will now analyze two possible roles of quasi-active membranes in performing specific types of operations in nerve cells. Both mechanisms might be used in the vertebrate retina.

6 Temporal Differentiation

The differentiation of a function in the time domain corresponds to the multiplication of the Fourier transformed function with the frequency variable, i.e.

$$\frac{df(t)}{dt} \to i\omega \tilde{f}(\omega). \tag{16}$$

If the frequency components above the resonant frequency are disregarded, the highpass component of the transfer function of Fig. 6 can be approximated by

$$|\tilde{K}(x, \omega)| = a + b\omega \tag{17}$$

with a and b positive constants and $b > a$. Injecting a current $I(t)$ containing no frequency components above f_{max} into the cable leads therefore to a change in potential

$$V(t) = aI(t) + b\frac{dI(t)}{dt}. \tag{18}$$

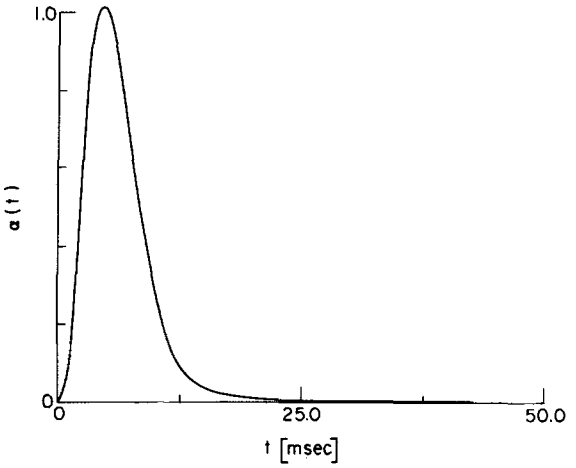

Fig. 12. The current input function used: $I(t) = \text{const} \cdot t^4 e^{-4t/t_{peak}}$. The current reaches its peak at 5 ms and has decayed to 1% of its peak value at about 16.9 ms. The scale of the ordinate is in arbitrary units. The Fourier transform $\tilde{I}(\omega)$ is proportional to $(i\omega + 4/t_{peak})^{-5}$ and has dropped to 52% of its steady-state value at 70 Hz, the resonant frequency of $\tilde{K}(x, \omega)$

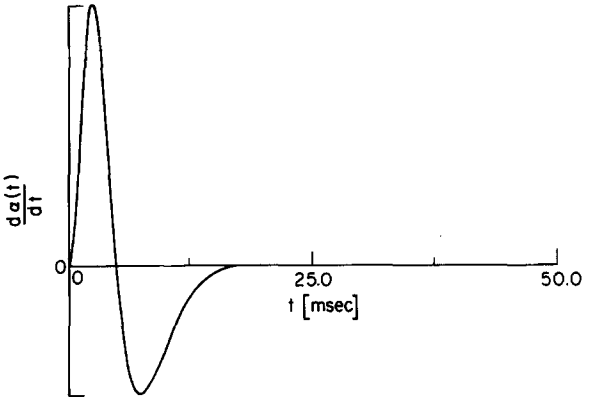

Fig. 13. The temporal derivative of Fig. 13

If $b \gg a$ (i.e. $q \to \infty$) the term proportional to the input can be neglected and the voltage is proportional to the temporal derivative of the current. In a more realistic situation there will be two sources of error. First, since the input function usually does contain frequency components beyond f_{max}, the fast components in the input function distort the derivative. Second, due to the non-zero steady state impedance $\tilde{K}(x, 0)$, stationary and slow inputs will not be filtered out completely as they should be. We demonstrated the feasibility of performing this operation using an infinite cable with a linearized Hodgkin-Huxley type membrane (such a system can be realized by small, subthreshold current stimuli in an axon). As current input we have used the generalized alpha function

$$I(t) = \text{const} \cdot t^4 e^{-4t/t_{peak}}$$

(see Fig. 12). Figure 13 shows the temporal derivative of the current. Injecting such a current with $t_{peak} = 5$ ms

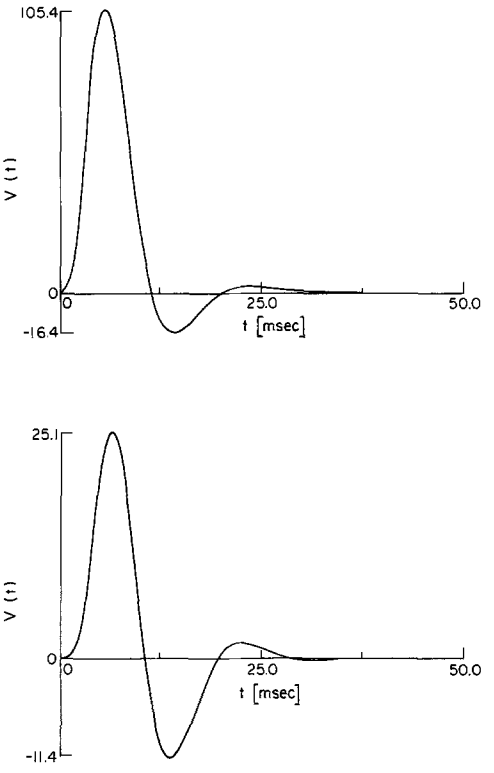

Fig. 14. The voltage in an infinite cable with a quasi-active membrane when an current of the form of Fig. 12 is injected and the voltage is recorded at the site of injection (top) or 350 µm farther away (bottom). In the first (respectively, second) case the voltage hyperpolarizes at about 11.3 ms (respectively, 10.5 ms) after the onset of current. The ordinate is in arbitrary units. If the current (Fig. 12) is choosen to have a maximal value of 10^{-7} A the voltage has a peak depolarization of 10.54 mV for the top figure and 2.51 mV for the bottom figure

into the cable and recording the voltage at the site of current injection and 350 µm farther away leads to the voltage profiles shown in Fig. 14. Clearly the general shape and behaviour of the voltage is in good qualitative agreement with the derivative of the input. The maximal depolarization decreases with the rise-time (t_{peak}) of the input while the time at which the potential first reverses increases with t_{peak}. Due to the bandpass nature of the membrane this reversal time decreases with increasing distance x (Detwiler et al., 1978). For a true differentiation, however, reversal of the potential should occur at t_{peak} and there should be no third, overbounding phase (which becomes increasingly dominant at increasing distances). The degree to which the voltage can be approximated as the derivative of the injected current depends on the time-course of $I(t)$. A faster rising input will have more high frequency components lying beyond f_{max} than a more slowly rising input. Lowering or increasing the leakage resistance r_{leak} of the membrane, will likewise lead to a better or worse approximation by varying the constant offset a in (18).

7 Spatio-Temporal Filtering

A rarely addressed issue is whether the receptive field of a retinal or cortical neuron changes its dimensions with changing temporal frequency of the visual stimulus. In particular, how does the shape of the spatial contrast sensitivity curve vary with the temporal frequency of the sinusoidal grating pattern drifting past the neuron's receptive field? For the simplest model of the receptive field the amount of attenuation the electric signal experiences between the site of synaptic input and the soma may be at least partially responsible for the dimensions of the receptive field. Since the amount of this attenuation is crucially dependent on the type of membrane present, different types of membranes lead to differing receptive fields. Increasing the temporal frequency of the presynaptic signal in a neuron with a purely passive dendritic tree, results in a postsynaptic signal containing increasingly higher frequency components. Accordingly, more and more charge leaks through the membrane and the dimensions of the receptive field decrease. We have demonstrated the feasibility of this mechanism in the case of cat retinal ganglion cells. On the basis of histological material provided by Boycott and Wässle (1974), we modeled the electrical behaviour of ganglion cells by approximating the whole dendritic tree in terms of cylindrical segments as described in detail elsewhere (Koch et al., 1982). Using the transmission line formalism (see Sect. 2) we designed an algorithm which automatically generates the transfer function $\tilde{K}_{ij}(\omega)$ for a current injection at site i and a voltage recording electrode at j in a structure of arbitrary geometry and linear membrane (Koch and Poggio, 1983b).

The voltage attenuation for an arbitrary input, current injection or conductance change, between the site of the synapse i and the soma s is the ratio of the voltage at the soma to the voltage at the synapse, i.e.

$$A_V(\omega) = \frac{\tilde{K}_{is}(\omega)}{\tilde{K}_{ii}(\omega)}, \tag{19}$$

where $\tilde{K}_{ii}(\omega)$ is the amplitude of the synaptic input impedance at the site of the synapse and $\tilde{K}_{is}(\omega)$ the amplitude of the transfer impedance between the synapse and the soma (Koch et al., 1982, 1983). In order to visualize the receptive field dimensions of these ganglion cells for different frequencies, we determine that region of the dendritic tree within which the voltage attenuation to the soma is always below a given constant factor C. Outside this region, synaptic inputs are attenuated by at least a factor C. Figure 15 shows the resulting picture in the case of a passive membrane for stationary and transient ($f = 100$ Hz) inputs where we choose as limiting values $C = 4$; i.e. 25% voltage attenuation. Clearly, the degree to which a synapse influences the somatic potential (and therefore the firing frequency) decreases at increasing frequencies. The particular values of the membrane leakage resistance ($r_{\text{leak}} = 3333\,\Omega\,\text{cm}^2$) and capacity ($c = 1\,\mu\text{F cm}^{-2}$) were chosen to illustrate this point and are not critical

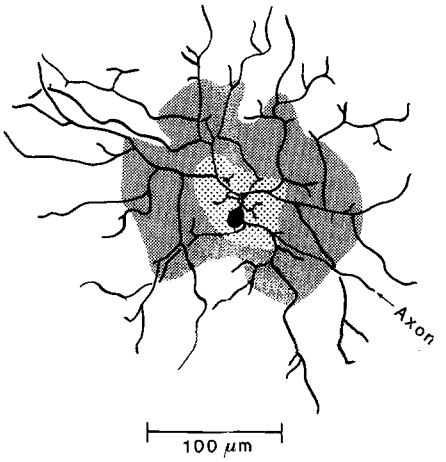

Fig. 15. Voltage attenuation in a cat retinal ganglion cell of the δ type (Boycott and Wässle, 1974). Such a cell was modeled using some 120 cylinders of varying lengths, diameters and membrane characteristics (for the detailed procedure see Koch et al., 1982). The large heavily dotted area indicates the region *within* which the voltage attenuation for stationary inputs from the synapse to the soma is less than a factor 4; i.e. the somatic voltage will be at least 25% of the voltage at the synaptic site. The smaller lightly dotted area illustrates the same concept for a sinusoidal input of 100 Hz frequency. The membrane is a passive one with $r_{\text{leak}} = 3333\,\Omega\,\text{cm}^2$ and $c = 1\,\mu\text{F cm}^{-2}$. (Adapted from Koch et al., 1983)

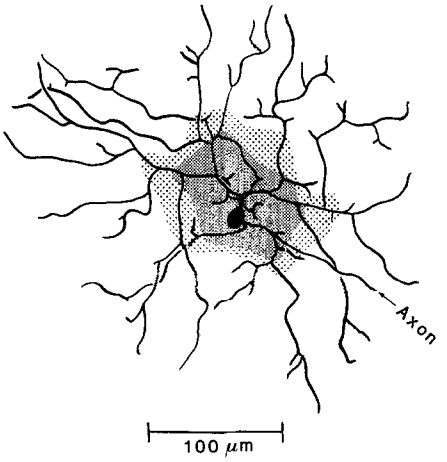

Fig. 16. The voltage attenuation for stationary (small heavily dotted area) and sinusoidal inputs (100 Hz; large lightly dotted area) in the cell of Fig. 15 with a quasi-active membrane. The membrane is of the linearized Hodgkin-Huxley type with the same leakage resistance and membrane capacity as in Fig. 15. Therefore Fig. 15 can be considered a special case of the quasi-active case with negligeable active channel density. For a sinusoidal varying input of frequency above 200 Hz, the region of small attenuation will be less than the corresponding stationary region

for this mechanism. Increasing the resistance r_{leak} to $8000\Omega\,cm^2$ decreases the attenuation for inputs at the pheriphery to a few percent.

If the same operation is performed for the ganglion cell using a quasi-active membrane, the situation reverses. For a sinusoidal varying input of 100 Hz the voltage attenuation is markedly less than the attenuation for stationary inputs (Fig. 16); under these conditions transient inputs influence the somatic potential more strongly than slowly changing inputs. As a consequence, such a cell responds in a given experimental situation preferentially to transient than to steady-state stimuli (Derrington and Lennie, 1982; Enroth-Cugell et al., 1983).

8 Discussion

The rationale behind our study is to begin to explore some of the theoretical possibilities for information processing in single neurons opened up by recent findings concerning the existence and distribution of voltage-, time-, and neurotransmitter-dependent channels. In general the underlying mechanism, i.e. the dependence of the channel conductance on transmembrane voltage and time, is complicated and nonlinear. Therefore we have restricted ourselves in this first analysis to a less ambitious goal: if the membrane voltage does not stray too far away from a given potential $\bar{V}$ (for example the resting potential of the cell) the voltage dependence of the channel conductance can be neglected and we need only concern ourselves with the time dependence. This is achieved by linearizing the channel kinetics around $\bar{V}$. Within the range of validity of the linear approximation the membrane can be described and analyzed in terms of a linear electric circuit containing resistances, inductances and capacitances. A dendrite or an extended dendritic structure endowed with a linearized membrane is amenable to an application of linear cable theory. Using an extension of classical cable theory to general linear membranes as our main tool, we inquire into the functional consequences of linearized membranes for the electric behaviour of neurons.

8.1 The Neuronal Membrane as a RLC Circuit

If the membrane channel conductance can be described by one or several auxiliary activation or inactivation variables, each governed by a first order differential equation, the linearized impedance for each variable can either be modeled as an inductive branch, i.e. an inductance in series with a resistance, or as capacitive branch, i.e. a capacity in series with a resistance. Both branches are shunted by an additional resistance which are combined with the leakage resistance and need not concern us further. It is only fair to add that these are not the only two possible circuits. The specific conditions under which an inductance or a capacity arise are given in Sects. 3.1 and 4.1. An example of a description using an inductive branch is the low threshold calcium mediated current in thalamic and inferior olivary neurons (Llinas and Yarom, 1981; Llinas and Jahnsen, 1982) or the calcium initiated potassium current in sympathetic neurons (Adams et al., 1982). A capacitance arises when the high threshold, non-inactivating calcium current in the cerebellum and hippocampus (Llinas and Sugimori, 1980; Schwartzkroin and Slawsky, 1977) is linearized.

8.2 How Valid is the Linear Description?

In discussing the question of the validity of the linear approximation we have to distinguish carefully between two different, but related concepts. On the one hand we can ask how valid the linear approximation of the channel conductance is: in comparing the response of the linear system to the response of the nonlinear membrane, one would like to know by how much they differ. On the other hand we can inquire for what values of $\bar{V}$ a linear description is at all possible. Clearly there must be a range of voltages, for instance in the neighbourhood of the threshold for generating spikes, where linearization leads to an unstable system (Sect. 5.1). While it is possible to respond to the last question in a precise sense (see Fig. 10) the former lacks an equally precise answer.

The linear description, assuming for the moment that it does exist, is only valid for "small" excursions of voltage δV away from $\bar{V}$. If δV increases, the response of the linear system deviates more and more from the solution of the nonlinear system. The difficulty lies in trying to make the term "small" precise. We can regard, however, the threshold for eliciting strong nonlinear electric events, like spikes, as an upper bound for the range of validity of the linear approximation. Therefore, for systems with a low threshold the linear description might only be valid for voltage displacements of 1 or 2 mV away from $\bar{V}$ while membranes with a higher threshold can be approximated within a larger voltage range by a linear membrane. Sabah and Leibovic (1969) and Mauro and collegues (1970) have studied this problem in the case of the linearized Hodgkin-Huxley equations. Comparing the small-signal analysis of the squid axon with the full system shows that the linear approximation reproduces satisfactorily the nonlinear response for current steps in the range of 4–5 mV around the resting potential. Reducing the density of active channels does lead to an increased range of validity as witnessed by the reduced degree of regeneration and finally, below a critical density, by the absence of spikes

altogether (Cooley and Dodge, 1966; Sabah and Leibovic, 1972).

For non-spiking neurons (see Roberts and Bush, 1981 for a thorough coverage of this subject) a linear description is likely to be more appropriate than in other systems because these neurones use decrementing, graded potentials with amplitudes one or two order of magnitude smaller than the 100 mV spike. Some of the cells are known, however, to possess fast Na^+, TTX sensitive channels (Hengstenberg, 1977; Mirolli, 1981) or Ca^{2+} dependent regenerative responses (Johnston and Lam, 1981). In the rod network of the turtle (Detwiler et al., 1978, 1980) and of the toad (Torre and Owen, 1983) the theoretical response predicted by the linear resonant model incorporating an inductive branch into the membrane of the rod is in good agreement with the hyperpolarizing voltage response to light below 5–6 mV. In turtle hair cells the change in membrane voltage caused by injections of rectangular current pulses is fitted by a linear (bandpass) model for depolarizations up to 20 mV and hyperpolarizations up to 30 mV in amplitude (Crawford and Fettiplace, 1981). We conclude that in systems with spike-like electrical activity the quality of the linear approximation is constrained by the threshold for generating spikes to voltage excursions of the order of a few mV around the resting potential while for non-spiking neurons with graded, electrotonic potentials the voltage range might be considerable higher.

Touching briefly the subject of the validity of the linear description, we consider the case of an imposed, long lasting current step. The membrane will depolarize to some new voltage value and reach its steady-state configuration. Will the corresponding linear model still be stable? As we have shown in Fig. 10 for the linearized Hodgkin-Huxley equations, it will be if the new imposed voltage is below $\bar{V}_{crit} = 6.24$ mV. At this potential the axon will show oscillatory responses (Sabah and Spangler, 1970) while the linear system displays run-away solutions, i.e. the voltage increases indefinetely with time. For membranes with a reduced channel population, $\bar{V}_{crit}$ increases until for values of η below 0.185 a stable linear description is always possible. We cannot generalize these results except in as far as the threshold for spikes will be proportional to $\bar{V}_{crit}$. The higher the threshold the larger the voltage domain for which a stable, linear description is possible.

8.3 Functional Consequences of a Capacitive Branch

What are the implications of a phenomenological capacitance for information processing? Introducing an extra capacitance by linearizing an appropriate voltage-dependent channel does not change the fundamental nature of the membrane but increases its time constant. This may be reflected in an increased delay for IPSP's and EPSP's propagating through the neuronal structure. In a dendritic tree with this type of membrane the rise time of an EPSP generated in the periphery and travelling towards the soma could be substantially enhanced in comparison with the situation in a passive membrane. Increasing delays by increasing the total membrane capacity might be of particular interest in light of the very small variation of membrane capacity measured in nerve cells [values of c are tightly clustered around $1\,\mu F\,cm^{-2}$; see Brown et al. (1981)]. Since the size of the extra capacity is inversely proportional to channel density, cells with a low density of channels are attractive as the locus of the delay operation. Direction selectivity in the retina depends, for instance, on the precise temporal conjunction at the level of ganglion cells of different signals having delays up to 30 ms (Reichardt, 1961; Wyatt and Daw, 1975; Torre and Poggio, 1978; Marchiafava, 1979). These delays might possibly be obtained by the passage of the light-evoked signal through bipolar cells, believed to be non-spiking. Another example is the theoretically postulated (Richter and Ullman, 1982) and experimentally measured differential delay (with a median value of 3.4 ms) between the centre and surround pathway in cat X ganglion cells (Derrington and Lennie, 1982; Enroth-Cugell et al., 1983). Introducing a capacitive branch does have, however, a serious drawback: because more charge leaks through the membrane than in the passive case the space constant $\lambda(\omega)$ decreases. A way to circumvent this problem is an increase in the leakage resistance r_{leak} without any extra capacitive branch. This will actually enhance the space constant and therefore strengthen the influence of a synapse on the soma (Sect. 4.2). Given the large uncertitude regarding possible values for the leakage resistance (depending on the neuronal system anywhere between $500\,\Omega\,cm^2$ and $1\,M\Omega\,cm^2$) it seems much more likely that an increase in r_{leak}, rather than an additional capacity, would be used to create neuronal delay lines.

8.4 Functional Consequences of an Inductive Branch

General Properties. As we have seen before, adding an inductive branch to a lowpass membrane can give rise to novel properties. But under what conditions is the membrane impedance $z_m(\omega)$ a bandpass? We are able to prove that if the resistance r_l in series with the inductance (Fig. 2), or the leakage resistance r is sufficiently small, $z_m(\omega)$ behaves like a bandpass. The first condition can always be met if the time-constant of the channel (at a fixed potential) is very large, i.e. the conductance change occurs sufficiently slow (see end of

Appendix III). Apart from these two criteria for the occurance of a bandpass, relatively slow channel kinetics and low membrane resistance, the question can only be answered in a specific instance by performing the necessary linearization procedure.

The value of the resonant frequency depends on the linearized membrane. f_{max} may be as low as 1 Hz as in heart cell membrane (Clapham and DeFelice, 1982) or as high as several hundred Hz as in the frog node (Clapham and DeFelice, 1976). If $z_m(\omega)$ is a bandpass, or in physiological terms, if a small patch of membrane shows a bandpass-like behaviour, it follows necessarily from are theorem (Sect. 3.2) that the input-impedance $\tilde{K}(0, \omega)$, the transfer-impedance $\tilde{K}(x, \omega)$ for any x and the space constant $\lambda(\omega)$ in an infinite cable must also be bandpass functions. In other words, voltage recorded from such a cable will always show oscillatory components.

To explore some specific properties of quasi-active membranes we analyse the linearized Hodgkin-Huxley equations. We have choosen these equations because they represent one of the very few instances where the channel kinetics and the resulting electrical activity are completely captured in terms of four phenomenological variables. Let us then first consider the question of how the shape of the transfer-function $\tilde{K}(x, \omega)$, which determines the voltage response to a current input, is influenced by various biophysical parameters. As shown in Sects. 5.2 and 5.3 the resonant frequency is to a large extent independent of the diameter of the cable and of the distance between the site of current injection and voltage recording. It does, however, vary with the channel density η, increasing for a membrane with a higher population of active channels. q, the ratio between the peak amplitude and the steady-state amplitude, is very susceptible to changes in diameter, distance between the sites of input and output and channel density. It seems therefore possibly, given a thin neuronal process or a fiber heavily populated with active channels[5] to construct a filter where only components within a frequency band centered around f_{max} are passed while all other frequency components are filtered out.

We consider three specific instances where nerve cells with a quasi-active membrane can perform novel information processing tasks.

Electrical Tuning. Individual sensory neurons, converting sound pressure or electrical fields into spikes, have an optimal operating range in terms of the frequency of the input wave to which they are most sensitive. Such differential frequency tuning has been observed in hair cells of the vertebrate cochlea (for instance in turtle: Crawford and Fettiplace, 1980 and 1981 or in bullfrog: Lewis and Hedspeth, 1983; see also Ashmore, 1983) or in fish electroreceptors thought to derive from hair cells (Hopkins, 1976; Meyer and Zakon, 1982).

Hair cells, tonotopically organized along the basilar membrane in the cochela according to their characteristic frequencies (the frequency of the sound stimuli the cell optimally responds to), reveal their electrical tuning by damped oscillations of the membrane potential induced by current injections. The frequency of the induced oscillation coincides with the characteristic frequency. The basis of the tuning effect is believed to be an electrical resonance mechanism located in every hair cell (Crawford and Fettiplace, 1981). The question of the ionic nature of this mechanism has been addressed very recently by Lewis and Hudspeth (1983) using the Gigaseal whole-cell technique. They report the presence of three different types of channels (Ca^{2+}-, K^+-, and Ca^{2+} triggered K^+-conductances), one or several of them being most likely responsible for the tuning effect. In order to explain a) the large range (70–700 Hz) of the characteristic frequency shown by hair cells and b) the systematic variation of this frequency along the basilar membrane we propose that the nature of the individual channels remains invariant for all cells while the density of channels varies from cell to cell (see Crawford and Fettiplace, 1981 for a similar suggestion). Due to this varying channel density and the concomittant varying electrical excitability one would expect a correlation between the characteristic frequency of individual hair cells and their degree of nonlinearity. While this mechanism leads to a fixed, stable distribution of characteristic frequencies, short lasting effects might be achieved by a shift in the concentration of some ions like calcium (see Ashmore, 1983), neurotransmitters or even hormones such as experimentally induced in electric fish (Meyer and Zakon, 1982).

Temporal Differentiation. It would seem an attractive possibility if the central nervous system could perform differentiation-like operations. Of course we cannot expect a biological system to perform a precise mathematical differentiation, but we would like an approximation to this operation required for a variety of high-level tasks. Richter and Ullman (1982) have postulated that such an operation takes place at the level of the inner plexiform layer in the vertebrate retina. They suggested that the dyad, where the bipolar cell contacts the amacrine and the ganglion cell, together with the recurrent synapse from the amacrine cell back onto the bipolar, is responsible for the temporal differentiation of the bipolar intracellular voltage. A different mechanism operating in dendrites or axons with decremental electrotonic potentials and a sparse

5 There is evidence for an inverse relationship between the density of voltage dependent channels and the diameter of nerve fibers (Holden and Yoda, 1981; Smith and Schauf, 1981)

population of active channels, was suggested by Torre and Poggio (personal communication). Since the membrane impedance of such a structure has, to a first approximation, a constant positive slope from very low frequencies up to the resonant frequency, it can mimic a linear filter performing differentiation of its input. If current is injected into a cable with a quasi-active membrane, preferentially with a high q factor, the voltage recorded some distance away shows depolarizing and hyperpolarizing phases according to the rising and falling flanks of the input. Especially the time at which the potential reverses is directly proportional to the rise-time of the current pulse. Assuming linear interaction between synaptic inputs one can envisage a neuron with long and unbranched dendrites, like the γ ganglion cell of the cat retina (Boycott and Wässle, 1974) performing this differentiation on all its synaptic inputs, subsequently integrating the resulting graded potentials at the soma. The two important conditions for this kind of mechanism are a quasi-active membrane with a prominent maximum and modest, sub-threshold current input amplitudes.

Spatio-Temporal Filtering. Enroth-Cugell and Robson (1966) first measured the sensitivity function of cat ganglion cells by employing sinusoidal grating pattern drifting past the ganglion cell's receptive field. During these experiments the temporal frequency of stimulation remained always constant. Since that time only very little consideration has been given to the effect of temporal frequency on receptive field dimensions. Physiologists have only recently returned to this issue (Derrington and Lennie, 1982; Enroth-Cugell et al., 1983; for cat ganglion cells and Detwiler et al., 1978 and 1980 for the receptive fields of rods in the turtle). How does the receptive field vary with changing temporal frequency? In the simplest model for the receptive field we equate the extent of the receptive field with those synapses within the dendritic tree able to influence the somatic potential to a substantial degree. This notion presupposes some kind of topographical projection from the photoreceptors to the retinal neurons. If the influence of a synapse on the somatic potential is negligible, the corresponding presynaptic input will not contribute to the receptive field of the neuron. To give an exact and precise meaning to the notion of synaptic "influence" we introduce the voltage attenuation at a given frequency ω between the synaptic site i and the soma s [Eq. (19)]. Obviously, different types of membranes yield different degrees of voltage attenuation. To clarify this concept we determine for a cat retinal ganglion cell of the δ class (Boycott and Wässle, 1974) the region within which the voltage attenuation at a given temporal frequency is always below a given factor (25% in Figs. 15 and 16). In other words, the voltage attenuation between any synapse within this region and the soma is in no case larger than 4. For a passive membrane a faster and more rapid change in voltage will enhance this attenuation, i.e. reduce the region of low attenuation (Fig. 15). Thus, the synaptic weight of a particular synapse decreases with increasing transiency of its presynaptic input. If the ganglion cell is endowed with a quasi-active membrane incorporating a prominent inductance the situation reverses (at least for frequencies up to the resonant frequency): a given synapse can preferentially influence the somatic potential in a frequency band centered around f_{max} while it is less effective at lower and higher frequencies [see Fig. 5 in Enroth-Cugell et al. (1983) for some evidence of this; her finding that the extracellularly recorded response of X ganglion cells increases at higher temporal stimulus frequencies can also be explained, however, by the differential response of the photoreceptors and bipolar cells]. Interpreted in terms of receptive fields it follows that such a neuron integrates over a large area for rapid (but not too rapid) signals and over a smaller area for slow signals, as experimentally found in rods of the turtle (Detwiler et al., 1978, 1980). The data of Enroth-Cugell and colleagues do not support an analogous conclusion for X ganglion cells: while they measure some variation in the radius of the receptive field center as a function of the stimulus frequency (Fig. 7 in Enroth-Cugell et al., 1983) they did not observe a systematic variation common to all cells.

Interestingly, a recent theory of monocular depth perception explicitly requires a receptive field organization that decreases in size with increasing time, i.e. decreasing in size with decreasing temporal frequency (Buxton and Buxton, 1983).

8.5 Conclusion

We would like to end this paper with some speculations concerning the function of single neurons. Differing from the classical view where a neuron is considered mainly as threshold device, we picture a nerve cell as a complicated computational machine performing a variety of logical operations on its inputs. The basic units of information processing are patches of membranes, simple synaptic circuits or dendrites isolated from each other and from the soma (Schmitt et al., 1976; Poggio and Torre, 1981). Examples of these local circuits are the conjunction of a (shunting) inhibitory synapse with an excitatory one, mediating a highly selective veto operation (for a summary of this view see Swindale, 1983) or dendritic spines, possibly one of the elementary building blocks of memory (Koch and Poggio, 1983a). Applying this concept to the present study, we have to emphasize the analog aspects of the computations involved. Since there is no

clear all-or-none difference between a passive and a quasi-active membrane any type of binary information processing seems inappropriate. If graded, electrotonic potentials serve in some nerve cells (e.g. non-spiking neurons) as the main medium of signaling and information processing a variety of operations could be performed, in sharp contrast with the limited number of operations available if all-or-none, spike-like events are used as the elementary carriers of information. Multiplication- and division-like operations, integrating and differentiating, direction selectivity and spatio-temporal filtering can be localized in small, specialized subunits of the nerve cell rather than requiring several or a large number of neurons if these operations are to be carried out using spike trains.

Appendix I

Properties of a Passive Membrane with an Inductive Branch

Consider the electric circuit shown in Fig. 2, consisting of an inductance l and resistance r_l, in parallel to a capacity c and shunted by a resistance r. The square of its impedance is given by

$$|z(\omega)|^2 = r^2 \frac{r_l^2 + \omega^2 l^2}{A\omega^4 + B\omega^2 + C} \tag{AI.1}$$

with $A=(crl)^2$, $B=l^2+(crr_l)^2-2cr^2l$, and $C=(r+r_l)^2$. Finding the extrema of this symmetric function, i.e.

$$\frac{\partial |z(\omega)|^2}{\partial \omega} = 0, \tag{AI.2}$$

yields two solutions

$$\omega = 0$$

and

$$\omega^4 + 2\left(\frac{r_l}{l}\right)\omega^2 + \text{const} = 0, \tag{AI.3}$$

where $\text{const} = (Br_l^2 - l^2C)/Al^2$. It is easy to show that this biquadratic equation has at most one solution for positive frequency values. The solutions of (AI.3) have the form

$$\omega_{\max} = \pm(-\tau_l^{-2} \pm (\tau_l^{-4} - \text{const})^{-1/2})^{-1/2} \tag{AI.4}$$

where τ_l is the time-constant of the inductive branch, i.e. $\tau_l = l/r_l$. If $\text{const} < 0$, $\omega_{\max}^2$ has always one negative and one positive solution. For $\text{const} > 0$ no real solution exists. Therefore, if $\text{const} < 0$, $|z(\omega)|^2$ has at most one extremum for positive frequencies, a maximum [because for very large frequencies $|z(\omega)|^2$ goes to zero due to the presence of the capacity]. In order for this maximum to exist, r_l must obey $\text{const} < 0$, i.e. the following relation

$$\left(\frac{c}{l}\right)^2 r_l^4 - 2\left(\frac{c}{l}\right) r_l^2 - 2\left(\frac{1}{r}\right) r_l - 1 < 0. \tag{AI.5}$$

This fourth-degree polynomial is negative for a range of r_l-values between 0 and some positive, finite $r_{l,\text{crit}}$. Notice, that due to the $1/r$-term, $r_{l,\text{crit}}$ decreases for increasing leakage resistance r. For $r_l = 0$, i.e. the ideal resonant circuit, $f_{\max} = (lc)^{-1/2}$. For increasing r_l, const becomes more negative leading to a higher $\omega_{\max}$ until const reaches its minimum. Subsequent increase of r_l decreases the resonant frequency until at $r_l = r_{l,\text{crit}}$, $\text{const} = 0$, and $\omega_{\max}$ merges into the extremum at $\omega = 0$. We conclude that for a range of r_l-values between 0 and $r_{l,\text{crit}}$ the membrane impedance peaks at some positive frequency with $q > 1$. The same can also be said for r, c, and l^{-1}: for sufficiently small values of the shunting resistance r, the membrane capacity c or for sufficiently large values of the inductance l, expression (AI.5) will always be negative.

If the passive RC-element in Fig. 2 is replaced by a general lowpass impedance $z_m(\omega)$, the argumentation is similar. Since $z_m(\omega) = a(\omega) + ib(\omega)$ has by definition, an extremum at $\omega = 0$ it follows that $a > 0$, $b = 0$, and $(da/d\omega) = 0$. The amplitude of the total membrane impedance is

$$|z(\omega)|^2 = \frac{(a^2+b^2)(r_l^2+\omega^2 l^2)}{(r_l+a)^2+(b+\omega l)^2}. \tag{AI.6}$$

It is straightforward to show that for a range of r_l-values between 0 and some non-zero value, $|z(\omega)|^2$ has one extremum at some positive frequency.

Appendix II

Bandpass Behaviour of a Linear, Infinite Cable

Given an infinite cable with constant diameter and a membrane characterized by the membrane impedance $z_m(\omega)$ with real- and imaginary-part $a(\omega)$ and $b(\omega)$, i.e. $z_m(\omega) = a(\omega) + ib(\omega)$. Assuming that this membrane impedance shows bandpass behaviour, we will prove that:

the input impedance $\tilde{K}(0,\omega)$ is also a bandpass with the same resonant frequency and vice versa,

the transfer function $\tilde{K}(x,\omega)$ for any x is a bandpass

the space constant $\lambda(\omega)$ is a bandpass.

Following Eq. (6) we obtain for the square of the amplitude of the input impedance

$$|\tilde{K}(0,\omega)|^2 = 0.25 r_a |z_m(\omega)|. \tag{AII.1}$$

Taking the first derivative with respect to frequency yields

$$\frac{\partial |\tilde{K}(0,\omega)|^2}{\partial \omega} = \frac{r_a}{4} \frac{\partial |z_m(\omega)|}{\partial \omega}. \tag{AII.2}$$

Therefore, if $z_m(\omega)$ has a peak at some frequency value $\omega_{\max}$, so does the input impedance and vice versa.

Because the steady state membrane impedance $z_m(\omega = 0)$ is purely ohmic and $z_m(\omega)$ is, like $\tilde{K}(x,\omega)$ and $\lambda(\omega)$, a symmetric function in ω, we make use of the following three relations:

$$a(\omega)|_{\omega=0} > 0 \qquad b(\omega)|_{\omega=0} = 0 \qquad a(\omega)'|_{\omega=0} = 0, \tag{AII.3}$$

where prime denotes differentiation with respect to ω. In order for $z_m(\omega)$ to be a bandpass, $|z_m(\omega)|$ must increase in some neighbourhood of zero. This is equivalent with demanding that the second derivative at $\omega = 0$ should be positive. We have then

$$\frac{\partial^2 |z_m(\omega)|^2}{\partial \omega^2} = \frac{\partial 2(a(\omega)a(\omega)' + b(\omega)b(\omega)')}{\partial \omega}$$
$$= 2(a(\omega)'^2 + a(\omega)a(\omega)'' + b(\omega)'^2 + b(\omega)b(\omega)''), \tag{AII.4}$$

where doubleprime denotes the second derivative with respect to ω. Evaluating this expression at $\omega = 0$ gives a necessary and sufficient requirement for $z_m(\omega)$ to be a bandpass

$$aa'' + b'^2 > 0 \tag{AII.5}$$

with $a = a(\omega = 0)$ and $b = b(\omega = 0)$. Since a and b'^2 are both positive, a sufficient condition is that the second derivative of $a(\omega)$ at $\omega = 0$ (a'')

be positive. Because of Eq. (AII.2) the same applies also to $\tilde{K}(0,\omega)$. Following Eq. (8), the frequency-dependent space constant can be written as

$$\lambda(\omega)^{-1}=\mathrm{Re}\left\{\left(\frac{a(\omega)-ib(\omega)}{a(\omega)^2+b(\omega)^2}\right)^{1/2}\right\}. \tag{AII.6}$$

Because $\mathrm{Re}\{(\alpha+i\beta)^{1/2}\}=(\alpha+(\alpha^2+\beta^2)^{1/2})^{1/2}2^{-1/2}$ if $\alpha>0$, we have

$$\lambda(\omega)=\left(\frac{a(\omega)^2+b(\omega)^2}{a(\omega)+(a(\omega)^2+b(\omega)^2)^{1/2}}\right)^{1/2}. \tag{AII.7}$$

A necessary and sufficient condition for $\lambda(\omega)$ to show bandpass behaviour is

$$\left.\frac{\partial^2\lambda(\omega)}{\partial\omega^2}\right|_{\omega=0}>0.$$

Evaluating this expression leads to

$$\left.\frac{\partial^2\lambda(\omega)}{\partial\omega^2}\right|_{\omega=0}=2^{-3/2}a^{-3/2}(aa''+1.5b'^2). \tag{AII.8}$$

Comparing this with Eq. (AII.5), it follows that the latter relation ($aa''+b'^2>0$) implies the former. The converse is, however, not necessarily true: knowing that $\lambda(\omega)$ is a bandpass does not imply that $\tilde{K}(0,\omega)$ must also be one.

For the last part of the proof, we make use of Eq. (9):

$$|\tilde{K}(x,\omega)|=|\tilde{K}(0,\omega)|e^{-x/\lambda(\omega)}.$$

Differentiating twice with respect to ω and evaluating the result at $\omega=0$ [taking into account that the first derivative of $\lambda(\omega)$ and $\tilde{K}(0,\omega)$ are zero at $\omega=0$] leads to

$$\left.\frac{\partial^2|\tilde{K}(x,\omega)|}{\partial\omega^2}\right|_{\omega=0}=(\tilde{K}(0,0)''+x\lambda(0)^{-2}\lambda(0)''\tilde{K}(0,0))e^{-x/\lambda(0)}. \tag{AII.9}$$

If we assume that the input-impedance is a bandpass, i.e. $\tilde{K}(0,0)''>0$, we know that $\lambda(0)''>0$ (see above). Because x is the distance between the sites of input and output, i.e. $x>0$, the whole expression (AII.9) will be positive and $\tilde{K}(x,\omega)$ is a bandpass. Unfortunately, the inverse does not hold. Evaluating (AII.9) in terms of a and b reduces to the relation

$$aa''+1.5b'^2>0.$$

From this we can only deduce that if $\lambda(\omega)$ is a bandpass so is $\tilde{K}(x,\omega)$ and vice versa.

Appendix III

Membrane Parameters for the Linearized, Hodgkin-Huxley Equations

The membrane current density I, for the squid giant axon modified by a variable channel density η [see (15)] may be written as (Hodgkin und Huxley, 1952)

$$I=c\frac{dV}{dt}+\eta\bar{g}_{\mathrm{Na}}m^3h(V-V_{\mathrm{Na}})+\eta\bar{g}_k n^4(V-V_K)+g_{\mathrm{leak}}(V-V_{\mathrm{leak}}), \tag{AIII.1}$$

where the variables m, n, and h are governed by three first-order differential equations:

$$\begin{aligned}\frac{dn}{dt}&=\alpha_n-(\alpha_n+\beta_n)n=\frac{n_\infty-n}{\tau_n},\\ \frac{dm}{dt}&=\alpha_m-(\alpha_m+\beta_m)m=\frac{m_\infty-m}{\tau_m},\\ \frac{dh}{dt}&=\alpha_h-(\alpha_h+\beta_h)h=\frac{h_\infty-h}{\tau_h},\end{aligned} \tag{AIII.2}$$

where the steady-state values and the time constants are related to the rate constants by $n_\infty=\alpha_n/(\alpha_n+\beta_n)$ and $\tau_n=1/(\alpha_n+\beta_n)$ etc., and the rate constants themselves depend only on voltage (for a precise description of this dependence see Hodgkin and Huxley, 1952). Linearization about the potential $\bar{V}$ leads to a description of the membrane conductance in terms of linear, voltage- and time-independent electrical elements. We will not go into the details of this procedure but simply give the resulting equations [for a detailed description of the linearization see Mauro et al. (1970) or Sabah and Leibovic (1969)]. The activating (m) Na^+-current is equivalent to a resistance

$$R^*_{\mathrm{Na}}=\frac{1}{\eta\bar{g}_{\mathrm{Na}}m^3h} \tag{AIII.3a}$$

in parallel with an inductive branch consisting of a resistance

$$r^*_m=\frac{\alpha_m+\beta_m}{3\eta\bar{g}_{\mathrm{Na}}m^2h(V-V_{\mathrm{Na}})\left(\frac{d\alpha_m}{dV}-m\frac{d(\alpha_m+\beta_m)}{dV}\right)} \tag{AIII.3b}$$

and an inductance

$$l^*_m=\frac{r^*_m}{\alpha_m+\beta_m}. \tag{AIII.3c}$$

As in all subsequent equations, the variables m, n, and h, and all rate-constants and their derivatives are evaluated at $\bar{V}$. Since for $V_{\mathrm{Na}}<\bar{V}<V_K$, r^*_m, and l^*_m are always negative, we convert these elements into a positive resistance r_m and positive capacity c_m, shunted by the negative resistance R_{Na}:

$$R_{\mathrm{Na}}=\frac{r^*_mR^*_{\mathrm{Na}}}{R^*_{\mathrm{Na}}+r^*_m}, \tag{AIII.4a}$$

$$r_m=-r^*_m, \tag{AIII.4b}$$

$$c_m=\frac{-l^*_m}{r^{2*}_m}. \tag{AIII.4c}$$

The inactivating (h) Na^+-current yields two positive elements: a resistance

$$r_h=\frac{\alpha_h+\beta_h}{\eta\bar{g}_{\mathrm{Na}}m^3(V-V_{\mathrm{Na}})\left(\frac{d\alpha_h}{dV}-h\frac{d(\alpha_h+\beta_h)}{dV}\right)} \tag{AIII.5a}$$

in series with an inductance

$$l_h=\frac{r_h}{\alpha_h+\beta_h}. \tag{AIII.5b}$$

The activating (n) K^+-current is described by three positive elements. An inductive branch

$$r_n=\frac{\alpha_n+\beta_n}{4\eta\bar{g}_k n^3(V-V_K)\left(\frac{d\alpha_n}{dV}-n\frac{d(\alpha_n+\beta_n)}{dV}\right)}, \tag{AIII.6a}$$

$$l_n=\frac{r_n}{\alpha_n+\beta_n} \tag{AIII.6b}$$

shunted by a resistance

$$R_K=\frac{1}{\eta\bar{g}_K n^4}. \tag{AIII.6c}$$

To arrive at the final representation of the membrane (Fig. 4), we combine the three shunting resistances into one new resistance r (with $r_{\mathrm{leak}}=1/g_{\mathrm{leak}}$)

$$1/r=1/r_{\mathrm{leak}}+1/R_{\mathrm{Na}}+1/R_K. \tag{AIII.7}$$

Since R_{Na} is negative [(AIII.4a)], r can also be negative. However, one requirement for a stable, linear system is that the total steady-state resistance be positive, i.e. $1/r+1/r_n+1/r_h>0$ (Sect. 5.1). Assuming a value of $3333.3\Omega\,cm^2$ for the membrane leakage resistance and $1\mu F\,cm^{-2}$ for the membrane capacity, the linearization around the membrane resting potential ($\bar{V}=0$) yields the following values (with $\eta=1$ and independent of the diameter): $r=4070.2\Omega\,cm^2$; $c=1\mu F\,cm^{-2}$; $r_m=2317.2\Omega\,cm^2$; $c_m=0.102\mu F\,cm^{-2}$; $r_n=1177.9\Omega\,cm^2$; $l_n=6.43\,H\,cm^2$; $r_h=13971.1\Omega\,cm^2$; $l_h=119.0\,H\,cm^2$. The intracellular resistance r_a was assumed to be $70\Omega cm$ (see also Sabah and Leibovic, 1969; Mauro et al., 1970). The resting potential of the ionic batteries were $V_{Na}=112.0\,mV$ and $V_K=-12.0\,mV$. The battery of the leakage resistance was adjusted to the variable channel density to retain the original resting potential of the cell:

$$V_{leak}=-\left(\frac{V_{Na}}{R_{Na}}+\frac{V_K}{R_K}\right)r_{leak}. \tag{AIII.8}$$

To understand how the circuit elements vary with changing time constants τ, we use the same kind of linearization procedure as above to define the impedance for the K^+ activation system in terms of the variables n_∞ and τ_n. This yields straightforwardly

$$r_n^{-1}=4\eta\bar{g}_K n^3(V-V_K)\left(\frac{dn_\infty}{dV}-\left(\frac{n_\infty-n}{\tau_n}\right)\frac{d\tau_n}{dV}\right), \tag{AIII.9a}$$

$$l_n=\tau_n r_n. \tag{AIII.9b}$$

If only the kinetics of the channels, without their voltage dependence, are changed, i.e. only τ_n, (AIII.9) can be written as

$$r_n=\frac{\tau_n}{\tau_n a+b}, \tag{AIII.10a}$$

$$l_n=\frac{\tau_n^2}{\tau_n a+b}, \tag{AIII.10b}$$

where the constant a is always positive (for the usual voltage range between V_K and V_{Na}) and b is positive for a depolarization and negative for a hyperpolarization. Hence, for very fast kinetics, both the resistance and the inductance will be very small and tend in the limit to zero. For increasing slower kinetics, r_n increases to a finite boundary value while the inductance increases without limit.

Acknowledgements. I gratefully acknowledge my intellectual debt to Prof. Tomaso Poggio and Dr. Vincent Torre. They pointed out to me the possibility of using quasi-active membranes to perform a temporal differentiation. Prof. Poggio also suggested the possible consequences of a quasi-active membrane for the receptive fields of retinal neurons. I am grateful to K. Nielsen, T. Poggio, I. Segev, V. Torre, and A. Yuille for critically reading the manuscript. The research described was done at the Max-Planck-Institut für biologische Kybernetik and at the Department of Psychology and the Artificial Intelligence Laboratory of the Massachusetts Institute of Technology. The author was supported by a fellowship from the Studienstiftung des deutschen Volkes and is presently supported by the Fritz Thyssen foundation.

References

Adams, P.R., Constanti, A., Brown, D.A., Clark, R.B.: Intracellular Ca^{2+} activates a fast voltage-sensitive K^+ current in vertebrate sympathetic neurones. Nature **296**, 746—749 (1982)

Ashmore, J.: Listening with one cell. Nature **304**, 489—490 (1983)

Barrett, E.F., Barrett, J.N., Crill, W.E.: Voltage-sensitive outward currents in cat motoneurones. J. Physiol. **304**, 251—276 (1980)

Boycott, B.B., Wässle, H.: The morphological types of ganglion cells of the domestic cat's retina. J. Physiol. **240**, 397—419 (1974)

Brown, D.A., Adams, P.R.: Muscarinic suppression of a novel voltage-sensitive K^+-current in a vertebrate neurone. Nature **283**, 673—675 (1980)

Brown, T.H., Perkel, D.H., Norris, J.C., Peacock, J.H.: Electrotonic structure and specific membrane properties of mouse dorsal root ganglion neurons. J. Neurophysiol. **45**, 1—15 (1981)

Brühl, G., Jansen, W., Vogt, H.-J.: Nachrichtenübertragungstechnik. Stuttgart: Kohlhammer Verlag 1979

Buxton, B.F., Buxton, H.: Monocular depth perception from optical flow by space time signal processing. Proc. R. Soc. London B**218**, 27—47 (1983)

Chandler, W.K., Fitzhugh, R., Cole, K.S.: Theoretical stability properties of a space-clamped axon. Biophys. J. **2**, 105—127 (1962)

Clapham, D.E., DeFelice, L.J.: The theoretical small signal impedance of the frog node, Rana pipiens. Pflügers Arch. **366**, 273—276 (1976)

Clapham, D.E., DeFelice, L.J.: Small signal impedance of heart cell membranes. J. Membrane Biol. **67**, 63—71 (1982)

Cole, K.S.: Rectification and inductance in the squid giant axon. J. Physiol. **25**, 2951 (1941)

Cole, K.S., Baker, R.F.: Longitudinal impedance of the squid giant axon. J. Gen. Physiol. **24**, 771—788 (1941)

Connors, B.W., Gutnick, M.J., Prince, D.A.: Electrophysiological properties of neocortical neurons in vitro. J. Neurophysiol. **48**, 1302—1420 (1982)

Cooley, J.W., Dodge, F.A., Jr.: Digital computer solutions for excitation and propagation of the nerve impulse. Biophys. J. **6**, 583—599 (1966)

Crawford, A.C., Fettiplace, R.: The frequency selectivity of auditory nerve fibres and hair cells in the cochlea of the turtle. J. Physiol. **306**, 79—125 (1980)

Crawford, A.C., Fettiplace, R.: An electrical tuning mechanism in turtle cochlear hair cells. J. Physiol. **312**, 377—412 (1981)

Crill, W.E., Schwindt, P.C.: Active currents in mammalian central neurons. Trends Neurosci. **6**, 236—240 (1983)

DeHaan, R.L., DeFelice, L.J.: Oscillatory properties and excitability of the heart cell membrane. In: Theoretical chemistry, periodicities in chemistry and biology. pp. 181—233. Eyring, H., Henderson, D. (eds.). New York: Academic Press 1978

Derrington, A.M., Lennie, P.: The influence of temporal frequency and adaptation level on receptive field organization of retinal ganglion cells in cat. J. Physiol. **33**, 343—366 (1982)

Detwiler, P.B., Hodgkin, A.L., McNaughton, P.A.: A surprising property of electrical spread in the network of rods in the turtle's retina. Nature **274**, 562—565 (1978)

Detwiler, P.B., Hodgkin, A.L., McNaughton, P.A.: Temporal and spatial characteristics of the voltage response of rods in the retina of the snapping turtle. J. Physiol. **300**, 213—250 (1980)

Eisenberg, R.S., Johnson, E.A.: Three-dimensional electrical field problems in physiology. Prog. Biophys. Mol. Biol. **20**, 1—65 (1970)

Enroth-Cugell, C., Robson, J.G.: The contrast sensitivity of retinal ganglion cells of the cat. J. Physiol. **187**, 517—552 (1966)

Enroth-Cugell, C., Robson, J.G., Schweitzer-Tong, D.E., Watson, A.B.: Spatio-temporal interactions in cat retinal ganglion cells showing linear spatial summation. J. Physiol. **341**, 279—307 (1983)

Gustafsson, B., Galvan, M., Grafe, P., Wigström, H.: A transient outward current in a mammalian central neurone blocked by 4-aminopyridine. Nature **299**, 252—254 (1982)

Halliwell, J.V., Adams, P.R.: Voltage-clamp analysis of muscarinic excitation in hippocampal neurons. Brain Res. **250**, 71—92 (1982)

Hengstenberg, R.: Spike responses of "non-spiking" visual interneurone. Nature **270**, 338—340 (1977)

Hodgkin, A.L., Huxley, A.F.: A quantitative description of membrane current and its application to conduction and excitation in nerve. J. Physiol. **117**, 500—544 (1952)

Holden, A.V., Yoda, M.: The effect of ionic channel density on neuronal function. J. Theor. Neurophysiol. **1**, 60–81 (1981)

Hopkins, C.D.: Stimulus filtering and electroreception: Tuberous electroreceptors in three species of gymnotoid fish. J. Comp. Physiol. **111**, 171—207 (1976)

Johnston, D., Lam, D.M.-K.: Regenerative and passive membrane properties of isolated horizontal cells from a teleost retina. Nature **292**, 451—453 (1981)

Koch, C.: Nonlinear information processing in dendritic trees of arbitrary geometries. Ph. D. Thesis, University of Tübingen (1982)

Koch, C., Poggio, T.: A theoretical analysis of electrical properties of spines. Proc. Roy. Soc. London B**218**, 455—477 (1983a)

Koch, C., Poggio, T.: A simple algorithm for solving the cable equation in dendritic trees of arbitrary geometry. Submitted (1983b)

Koch, C., Poggio, T.: Velocity: its meaning and application to one-dimensional cables (in preparation) (1984)

Koch, C., Poggio, T., Torre, V.: Retinal ganglion cells: A functional interpretation of dendritic morphology. Phil. Trans. R. Soc. London B**298**, 227—264 (1982)

Koch, C., Poggio, T., Torre, V.: Nonlinear interaction in a dendritic tree: localization, timing and role in information processing. Proc. Natl. Acad. Sci. USA **80**, 2799—2802 (1983)

Korn, G.A., Korn, T.M.: Mathematical handbook for scientists and engineers. New York: McGraw-Hill 1961

Lewis, R.S., Hudspeth, A.J.: Voltage- and ion-dependent conductances in solitary vertebrate hair cells. Nature **304**, 538—541 (1983)

Llinas, R., Jahnsen, H.: Electrophysiology of mammalian thalamic neurones in vitro. Nature **297**, 406—408 (1982)

Llinas, R., Sugimori, M.: Electrophysiological properties of in vitro Purkinje cell dendrites in mammalian cerebellar slices. J. Physiol. **305**, 197—213 (1980)

Llinas, R., Yarom, Y.: Properties and distribution of ionic conductances generating electroresponsiveness of mammalian inferior olivary neurones in vitro. J. Physiol. **315**, 569—584 (1981)

Marchiafava, P.L.: The responses of retinal ganglion cells to stationary and moving visual stimuli. Vision Res. **19**, 1203—1211 (1979)

Mauro, A., Conti, F., Dodge, F., Schor, R.: Subthreshold behavior and phenomenological impedance of the squid giant axon. J. Gen. Physiol. **55**, 497—523 (1970)

Meyer, J.H., Zakon, H.H.: Androgens alter the tuning of electroreceptors. Science **217**, 635—637 (1982)

Mirolli, M.: Fast inward and outward current channels in a non-spiking neurone. Nature **292**, 251—253 (1981)

Moore, L.E., Tsai, T.D.: Ion conductances of the surface and transverse tubular membranes of skeletal muscle. J. Membrane Biol. **73**, 217—226 (1983)

Poggio, T., Torre, V.: A theory of synaptic interactions. In: Theoretical approaches to neurobiology, pp. 28—38. Reichardt, W.E., Poggio, T. (eds.). Cambridge, NJ: MIT Press 1981

Rall, W.: Core conductor theory and cable properties of neurons. In: Handbook of physiology, pp. 39—97. Kandel, E., Geiger, S. (eds.). Washington, DC: American Physiological Society 1977

Reichardt, W.: Autocorrelation: a principle for the evaluation of sensory information by the central nervous system. In: Sensory communication, pp. 303—318. Rosenblith, W.A. (ed.). Cambridge, NJ: MIT Press 1961

Richter, J., Ullman, S.: A model for the temporal organization of *X*- and *Y*-type receptive fields in the primate retina. Biol. Cybern. **43**, 127—145 (1982)

Rinzel, J.: Integration and propagation of neuroelectric signals. In: Studies in mathematical biology, pp. 1—66. Levin, S.A. (ed.). Math. Assoc. America (1978)

Roberts, A., Bush, B.M.H.: Neurones without impulses: their significance for vertebrate and invertebrate nervous systems. Cambridge, NJ: Cambridge University Press 1981

Sabah, N.H., Leibovic, K.N.: Subthreshold oscillatory responses of the Hodgkin-Huxley cable model for the squid giant axon. Biophys. J. **9**, 1206—1222 (1969)

Sabah, N.H., Leibovic, K.N.: The effect of membrane parameters on the properties of the nerve impulse. Biophys. J. **12**, 1132—1144 (1972)

Sabah, N.H., Spangler, R.A.: Repetitive response of the Hodgkin-Huxley model for the squid giant axon. J. Theor. Biol. **29**, 155—171 (1970)

Schmitt, F.O., Dev, P., Smith, B.H.: Electrotonic processing of information by brain cells. Science **193**, 114—120 (1976)

Schwartzkroin, P.A., Slawsky, M.: Probable calcium spikes in hippocampal neurons. Brain Res. **135**, 157—161 (1977)

Scott, A.C.: Effect of the series inductance of a nerve axon upon its conduction velocity. Math. Biosci. **11**, 277—290 (1971)

Sirovich, L., Knight, B.W.: On subthreshold solutions of the Hodgkin-Huxley equations. Proc. Natl. Acad. Sci. USA **74**, 5199—5202 (1977)

Smith, K.J., Schauf, C.L.: Size-dependent variation of nodal properties in myelinated nerve. Nature **293**, 297—299 (1981)

Swindale, N.V.: Anatomical logic of retinal nerve cells. Nature **303**, 570—571 (1983)

Torre, V., Owen, W.G.: High-pass filtering of small signals by the rod network in the retina of the toad, Bufo Marinus. Biophys. J. **41**, 305—324 (1983)

Torre, V., Owen, W.G., Sandini, G.: The dynamics of electrically interacting cells. IEEE Trans. Syst. Man, Cybern. (in press)

Torre, V., Poggio, T.: A synaptic mechanism possibly underlying directional selectivity to motion. Proc. R. Soc. London B**202**, 409—416 (1978)

Wong, R.K.S., Prince, D.A., Basbaum, A.I.: Intradendritic recordings from hippocampal neurons. Proc. Natl. Acad. Sci. USA **76**, 986—990 (1979)

Wyatt, H.J., Daw, N.W.: Directionally sensitive ganglion cells in the rabbit: specificity for stimulus direction, size and speed. J. Neurophysiol. **38**, 613—626 (1975)

Received: November 6, 1983

Dr. Christof Koch
Dept. of Psychology and
Artificial Intelligence Laboratory
Massachusetts Institute of Technology
545 Technology Square
Cambridge, MA 02139
USA